





One Metric to Measure them All: Localisation Recall Precision (LRP) for Evaluating Visual Detection Tasks

Kemal Oksuz[†] , Baris Can Cam , Sinan Kalkan[‡] , and Emre Akbas[‡] 

Abstract—Despite being widely used as a performance measure for visual detection tasks, Average Precision (AP) is limited in (i) including localisation quality, (ii) interpretability and (iii) applicability to outputs without confidence scores. Panoptic Quality (PQ), a measure proposed for evaluating panoptic segmentation (Kirillov et al., 2019), does not suffer from these limitations but is limited to panoptic segmentation. In this paper, we propose Localisation Recall Precision (LRP) Error as the performance measure for all visual detection tasks. LRP Error, initially proposed only for object detection by Oksuz et al. (2018), does not suffer from the aforementioned limitations and is applicable to all visual detection tasks. We also introduce Optimal LRP (oLRP) Error as the minimum LRP error obtained over confidence scores to evaluate visual detectors and obtain optimal thresholds for deployment. We provide a detailed comparative analysis of LRP with AP and PQ, and use 35 state-of-the-art visual detectors from four common visual detection tasks (i.e. object detection, keypoint detection, instance segmentation and panoptic segmentation) to empirically show that LRP provides richer and more discriminative information than its counterparts. Code available at: <https://github.com/kemaloksuz/LRP-Error>.

Index Terms—Localisation Recall Precision Average Precision Panoptic Quality Object Detection Keypoint Detection Instance Segmentation Panoptic Segmentation Performance Metric Threshold.



1 INTRODUCTION

Many vision applications require identifying objects and object-related information from images. Such identification can be performed at different levels of detail, which are addressed by different detection tasks such as “object detection” for identifying labels of objects and boxes bounding them, “keypoint detection” for finding keypoints on objects, “instance segmentation” for identifying the classes of objects and localising them with masks, and “panoptic segmentation” for classifying both background classes and objects by providing detection ids and labels of pixels in an image. Accurately evaluating performances of these methods is crucial for developing better solutions.

Today “average precision” (AP), the area under the Precision-Recall (PR) curve, is the de facto standard for evaluating performance on many visual detection tasks and competitions [1], [2], [3], [4], [5], [6], [7]. AP not only enjoys vast acceptance but also appears to be unchallenged. There has been only a few attempts on developing an alternative to AP [8], [9], [10]. Despite its popularity, AP has many limitations as we discuss below.

1.1 Important features for a performance measure

To facilitate our analysis of AP and other performance measures, we define three important features:

Completeness. Arguably, three most important performance aspects that an evaluation measure should take into

account in a visual detection task are false positive (FP) rate, false negative (FN) rate and localisation error. We call a performance measure “complete” if it precisely takes into account all three quantities.

Interpretability. Interpretability of a performance measure is related to its ability to provide insights on the strengths and weaknesses of the detector being evaluated. To provide such insight, the evaluation measure should ideally comprise interpretable components.

Practicality. Any issue that arises during practical use of a performance measure diminishes its practicality. This could be, for example, any discrepancy between the well-defined theoretical description of the evaluation measure and its actual application in practice, or any shortcoming that limits the applicability of the measure to certain scenarios.

1.2 Limitations of AP

Completeness. Localisation quality is only loosely taken into account in AP. Detections that meet a certain localisation criterion (e.g., intersection over union (IoU) over 0.50 in object detection) are treated equally regardless of their actual localisation quality. Further increase in localisation quality, for example, increasing the IoU of a true positive (TP) detection, does not change AP (Figure 1).

Interpretability. The AP score itself does not provide any insight in terms of the important performance aspects, namely, FP rate, FN rate and localisation error. One needs to inspect the PR curve and make additional measurements (e.g. average-recall (AR) or some kind of localisation quality) in order to comment on the weaknesses or strengths of a detector in terms of these aspects. Therefore, being an

All authors are at the Dept. of Computer Engineering, Middle East Technical University (METU), Ankara, Turkey. E-mail: {kemal.oksuz@metu.edu.tr, can.cam@metu.edu.tr, skalkan@metu.edu.tr, emre@ceng.metu.edu.tr}

[†] Corresponding author.

[‡] Equal contribution for senior authorship.

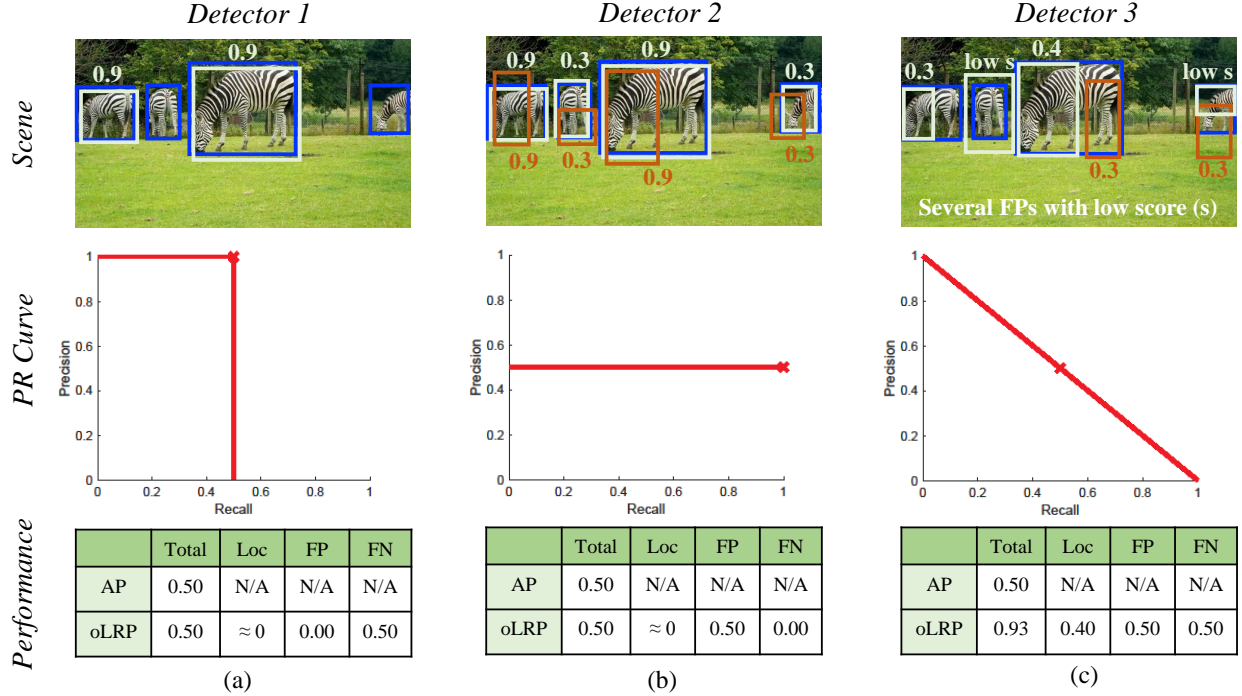


Fig. 1: Three different object detection results (for an image from COCO [1]) with very different PR curves but the same AP. **First Row:** Blue, white and orange colors denote ground-truth, TPs and FPs respectively. Numbers are confidence scores, s , of the detections. **Second row:** PR curves for the corresponding detections. Red crosses indicate optimal points designated by oLRP. **Third row:** AP and oLRP results of the detection results. Comparing LRP and AP, (i) In terms of “completeness” (Section 1.1): While the localisation quality of the TPs in (c) is worse than (a) and (b), AP does not penalize (c) more, while oLRP does. (ii) In terms “interpretability” (Section 1.1): AP is unable to identify the difference between (a) and (b) despite they have very different problems. On the other hand, oLRP, as an interpretable metric, demonstrates the strengths and weaknesses of each scenario with its components corresponding to each performance aspect.

approximation of the area under the PR curve, AP may fail to distinguish between the underlying issues of different detectors, as illustrated in Figure 1.

Practicality. We identify three major issues related to the practical use of AP:

(i) Using AP to evaluate hard-prediction tasks, i.e. tasks that involve outputs without confidence scores, such as panoptic segmentation [9], is problematic because hard predictions yield only a single point on the PR curve. Assumptions are needed to compute the area under the PR curve consisting of just one point.

(ii) AP cannot be used for model selection. For example, when a detector is to be deployed for a certain problem, an optimal detection threshold is needed. AP does not offer any help in finding such optimal thresholds.

(iii) Lastly, one needs to interpolate the PR curve before computing AP, which, as we will show, is a problem with classes with few examples.

We provide a detailed discussion on each limitation in Section 3 and provide an empirical analysis in Section 7.2.

1.3 Localisation Recall Precision (LRP) Error

LRP Error is a novel performance metric for visual detection tasks. We proposed LRP Error in our previous work [8] for the object detection task, where we showed that it alleviates all the aforementioned limitations of AP (Section 1.2): (i) LRP Error precisely combines the important performance aspects, therefore it is complete (compare AP and LRP in

Figure 1 - see Section 1.1 for completeness). (ii) LRP Error is easily interpretable by definition, and through its components, it provides insights regarding each performance aspect (compare AP and LRP in Figure 1). (iii) Regarding the practicality issues of AP; with the Optimal LRP (oLRP) extension, LRP Error can evaluate both soft predictions (i.e. outputs with class labels and confidence scores, such as in object detection) and hard predictions (i.e. outputs with class labels only, such as in panoptic segmentation), can provide a class-specific optimal threshold and does not employ any interpolation for its computation. In addition, LRP is a metric, for which, however, we do not demonstrate any theoretical or practical benefits.

1.4 Other alternatives to AP

While AP is still de facto performance measure for many visual detection tasks, recently proposed visual detection tasks have preferred not employing AP, but instead introduced novel performance measures:

Panoptic Quality (PQ): Panoptic segmentation task [9] requires the background classes to be labeled and localised by masks in addition to the objects. Since this task is a combination of the instance segmentation and semantic segmentation tasks, AP can be used to evaluate performance. However, arguing the inconsistency between machines and humans in terms of perceiving the objects due to the confidence scores in the outputs, Kirillov et al. [9] preferred to

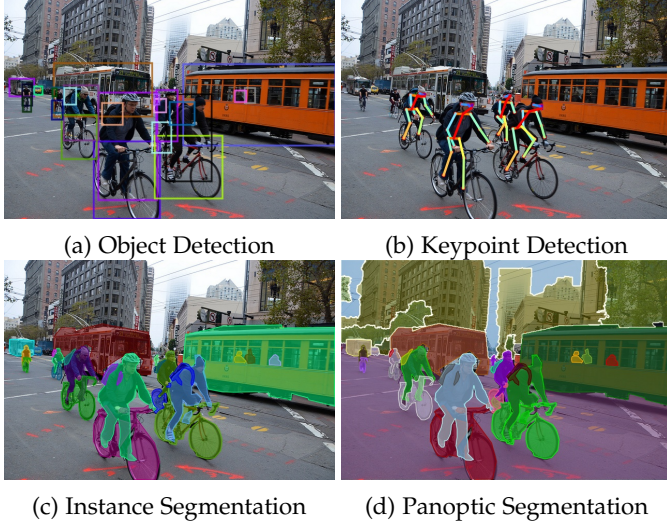


Fig. 2: The (visual) detection tasks considered in this paper. Keypoint detection is illustrated for the ‘person’ class. The image is taken from the COCO dataset [1]. Detectron2 [11] is used to plot the ground truths.

discard these scores for evaluation. Considering the limitations of AP to evaluate hard predictions (Section 1.2), PQ was proposed as a new performance measure to evaluate the results of the panoptic segmentation task. Similar to LRP Error [8], PQ combines all important performance aspects of visual detection, however, its extension to other visual detection tasks has not been explored. We provide a detailed analysis on PQ in Section 4 and discuss empirical results in Section 7.3. Note that PQ was proposed later than LRP.

Probability-based Detection Quality (PDQ): Unlike conventional object detection, probabilistic object detection (POD) [10] takes into account the spatial and semantic uncertainties of the objects, and accordingly for each detection, requires (i) a probability distribution over the class labels (i.e. instead of a single confidence score as in soft predictions) and (ii) a probabilistic bounding box represented by Gaussian distributions. Similar to Kirillov et al. [9], Hall et al. [10] also did not prefer an AP-based performance measure for POD, instead proposed a new performance measure called PDQ to evaluate probabilistic outputs. In this paper, we limit our scope to deterministic approaches to visual detection tasks. Therefore, we do not delve into a detailed discussion on PDQ as we do for AP and PQ; instead, we provide a guidance on how LRP Error can be extended for different visual detection tasks in Section 5.4.

1.5 Contributions of the Paper

Our contributions are as follows:

- 1) We thoroughly analyse Average Precision and Panoptic Quality.
- 2) We present LRP Error and describe its use for *all* visual detection tasks (Figure 2). LRP Error can evaluate all visual detection tasks in both output types (i.e. hard and soft predictions) by alleviating the drawbacks of AP and PQ. In particular, we empirically present the usage of LRP on four important visual detection tasks, namely, object detection,

keypoint detection, instance segmentation, panoptic segmentation, and discuss its potential extensions to other tasks.

- 3) While LRP Error can directly be used for hard predictions, to evaluate soft predictions we propose Optimal LRP (oLRP) error as the minimum achievable LRP Error over the confidence scores.
- 4) We show that LRP Error is an upper bound for the error versions of precision, recall and PQ (Section 6). Therefore, minimizing LRP is guaranteed to minimize the other measures.
- 5) We show that the performances of visual object detectors are sensitive to thresholding, and based on oLRP, we propose “LRP-Optimal Threshold” to reduce the number of detections in an optimal manner.

To demonstrate that LRP provides more insight than AP and PQ, we compare LRP with its counterparts on 35 state-of-the-art visual detectors. Using these detectors, we provide examples, observations and various analysis with LRP and oLRP at the detector- and class-level to present its evaluation capabilities. Our experiments also show that (i) LRP can unify the evaluation of all visual detection tasks in any desired output type (i.e. soft predictions or hard predictions), (ii) object detectors need to be thresholded in a class-specific manner, (iii) LRP-Optimal threshold is able to threshold object detectors a class-specific manner by considering all performance aspects, and (iv) the additional overhead of LRP computation to the COCO toolkit is negligible: It takes an additional 0.2 milliseconds per image on average (on COCO 2017 val) to output LRP, its components and LRP-Optimal thresholds on an eight-core standard CPU.

Comparison with Our Previous Work: The current paper extends our previous work [8] to *all* visual detection tasks. Hence, besides object detection, here, we present the usage of LRP on other three common visual detection tasks: (i) instance segmentation, (ii) keypoint detection and (iii) panoptic segmentation. While extending LRP for other detection tasks, we present how LRP can be employed to evaluate hard predictions, soft predictions and its potential extensions. Moreover, the experimental analysis is performed from scratch to cover all four detection tasks, to evaluate more recent detection methods, to dwell more on the analysis of oLRP and to investigate computational latency.

1.6 Outline of the Paper

The paper is organized as follows. Section 2 presents the related work. Sections 3 and 4 present a thorough analysis of Average Precision and Panoptic Quality respectively. Section 5 defines the LRP Error, oLRP Error and potential extensions of LRP. Section 6 compares LRP Error with AP and PQ. Section 7 presents several experiments to quantitatively analyse LRP. Finally, Section 8 concludes the paper.

2 RELATED WORK

Evaluation in visual detection tasks. As discussed in Section 1, except for the panoptic segmentation task which

uses PQ [9], the performances of visual object detection methods are conventionally evaluated using AP. Sections 3 and 4 discuss and present an analysis of these performance measures.

Another measure, PDQ [10] has recently been proposed for evaluating the probabilistic object detection task, where the label of a detection is represented by a discrete probability distribution over classes and the bounding boxes are encoded by Gaussian distributions. To compute PDQ, first, pairwise PDQ (pPDQ) score is computed over all detection-ground truth pairs and the optimal matchings are identified following the Hungarian Algorithm [12]. Then, determining TPs, FPs and FNs, and using the pPDQs of optimal matchings, PDQ score of a detection set can be computed by normalizing the sum of these pPDQs by the total number of TPs, FPs and FNs. To evaluate each pair, pPDQ combines localisation and classification performances by its spatial quality and label quality components. The spatial quality evaluates a pair in a pixel-based manner (i.e. not box-based) by exploiting the segmentation mask of the ground truth. And, the label quality of a pair is the probability of the ground truth label in the label distribution of the detection. Therefore, computing PDQ requires (i) segmentation masks which are normally not provided for the conventional object detection task, and (ii) the outputs to be in the described probabilistic form. In this paper, we demonstrate that LRP can be used for all common visual detection tasks having the conventional deterministic representation, and provide a guideline on how it can be employed by other tasks.

Analysis tools for visual detection tasks. Over the years, diagnostic tools have been proposed for providing detailed insights on the performances of detectors. For example, Hoiem et al. [13] selected the top-k FPs based on confidence scores and analysed them in terms of common error types (i.e. localisation error, confusion with similar objects, confusion with other objects and confusion with background). However, the tool of Hoiem et al. [13] requires additional analysis for FNs. Another toolkit, the COCO toolkit [1], is based on this analysis tool, but instead plots the considered error types on PR curves progressively to present how much AP difference is accounted by each error type. Recently, Bolya et al. [14] showed that the COCO toolkit can yield inconsistent outputs when the order of progressive contribution of the error types to the AP is interchanged. Moreover, this analysis by the COCO toolkit yields superimposed numerous PR curves which are time-consuming to examine and hard to digest. Based on these observations, Bolya et al. [14] proposed TIDE, a toolkit addressing the limitations of the previous analysis tools. TIDE introduces six different error types, each of which is summarized by a single score in the analysis result. Although such tools are useful for providing detailed insights on the types of errors detectors are making, they are not performance measures, and as a result they do not yield a single performance value as the detection performance.

Point multi-target tracking performance metrics. The evaluation of the detection tasks is very similar to that of multi-target tracking in that there are multiple instances of objects/targets to detect, and the localisation, FP and FN errors are common criteria for success. Currently, component-based performance metrics are the accepted way of eval-

uating point multi-target tracking methods. One of the first metric to combine the localisation and cardinality (including both FP and FN) errors is the Optimal Subpattern Assignment (OSPA) [15]. Among the successors of OSPA, our LRP [8] was inspired by the Deficiency Aware Subpattern Assignment metric [16], which combines the three important performance aspects.

Summary. We observe that, with similar error definitions, point multi-target tracking literature utilizes component-based performance metrics commonly, which has not been explored thoroughly in the visual detection literature. While a recent attempt, panoptic quality, is an example of that kind, it is limited to panoptic segmentation (Section 4). The analysis tools also aim to provide insights on the detector, however, a single performance value for the detection performance is not provided by these methods. In this paper, we propose a single metric that ensures important features (i.e. completeness, interpretability and practicality) while evaluating the performance of methods for visual detection tasks. We also show that our metric, considering all performance aspects, is able to pinpoint a class-wise optimal threshold for the visual detectors, from which several applications can benefit in practice.

3 AVERAGE PRECISION

This section provides a definition of AP and its detailed analysis.

3.1 Definition of AP

Computing AP for a class involves a set of detection results with confidence scores and a set of ground-truth items (e.g. bounding boxes in the case of object detection). First, detections are matched to ground-truth items (GT) based on a predefined spatial overlap criterion such as IoU¹ being larger than $\tau = 0.50$. Each GT can only match one detection and if there are multiple detections that satisfy the overlap criterion, the one with the highest confidence score is matched. A detection that is matched to a GT is counted as a TP. Unmatched detections are FPs and unmatched GTs are FNs. Given a specific confidence threshold s , detections with a lower confidence score than s are discarded, and TP, FP, FN values are calculated with the remaining detections as described. By systematically changing s , we obtain a precision-recall (PR) curve. This process usually results in a non-monotonic curve, that is, the precision may go up and down as recall is increased. Conventionally [1], [3], [7], [11], [17], in order to decrease these wiggles, the PR curve is interpolated as follows: denoting the precision at a recall r_i before and after interpolation by $p(r_i)$ and $\hat{p}(r_i)$ respectively, $\hat{p}(r_i) = \max_{r_j > r_i} p(r_j)$ [3]. Then, AP (for a class) is the area under this interpolated curve, or an approximation of this area by averaging it over evenly-spaced recall values [1], [3]. The detector's performance over all classes is obtained simply by averaging over AP values per class. In order to include the localisation quality, which is somewhat ignored by AP, the COCO-style AP, denoted by AP^C , computes

1. Note that while for the object detection task IoU is computed between bounding boxes, it is computed between the masks for segmentation tasks.

10 AP_τ where the TP validation threshold, τ , is increased between 0.50 and 0.95 with a step size of 0.05, and these 10 AP_τ values are averaged. From the definition of AP, it follows that it is a ranking-based performance measure, and favors methods that have high precision over the entire recall domain.

3.2 An Analysis of AP

In the following, we provide an analysis of AP by discussing its limitations introduced in Section 1.2 in detail:

Completeness. *AP does not explicitly evaluate localisation performance (Figure 1) and therefore, violates completeness.* To circumvent this issue, researchers typically use the following methods, neither of which ensures completeness:

- *Quantitatively using COCO-style AP (AP^C) or AP_τ with large τ :* AP variants do not include the precise localisation quality of a detection except for thresholding, hence the contribution of the localisation performance to these AP variants is always loose. Owing to this loose contribution, the localisation quality can not be quantified by AP. As a result, the methods specifically proposed to improve the localisation quality [18], [19], [20], [21], [22] have been struggling to present their contributions quantitatively. While some of them [21], [22] present only AP^C , AP_{75} and AP_{50} , a subset of these methods [18], [19], [20], [23] additionally resort to APs with larger τ values such as AP_{80} or AP_{90} . In any case, it is not clear or consistent to interpret any AP variant in terms of localisation.
- *Presenting qualitative examples [24], [25], [26], [27], [28], [29]:* In this case, note that it is very likely for the selected examples to be very limited and biased.

We empirically analyse this limitation in Section 7.2.1.

Interpretability. *The resulting AP value does not provide any insight on the strengths or weaknesses of the detector.* As illustrated in Figure 1, different detectors may yield different PR curves, highlighting different types of performance issues. However, being an approximation of the area under the PR curve, AP fails to distinguish between the underlying issues of different detectors. This is mainly because both precision and recall performances of a detector are vaguely combined into a single performance value as an AP value. Besides, interpreting the COCO-style AP, AP^C , is more difficult since the localisation quality is also integrated in an indirect and loose manner, resulting in an ambiguous contribution of important performance aspects, where it is not clear how much each aspect affects the resulting single performance value. Similar to our previous work [8], Bolya et al. [14] also criticized AP since it does not isolate error types. To alleviate this, the COCO toolkit [1] can output PR curves with an error analysis, which requires manual inspection of several superimposed PR curves in order to understand the strengths and weaknesses. This is, however, time-consuming and impractical with large number of classes such as the LVIS dataset [7] with around 1000 classes (also see the discussion on analysis tools in Section 2).

We empirically analyse this limitation in Section 7.2.2.

Practicality. One can also face some practical challenges while employing AP for some use-cases:

- *Evaluation of hard predictions with AP, though possible, is problematic.* Note that a hard prediction (i.e. an output without confidence score) corresponds to a single point on the PR space, hence determines a step PR curve resulting in $AP = \text{Precision} \times \text{Recall}$. However, AP intends to prioritize and rank the detections with respect to their confidence scores, which are not included in hard predictions. As a result, in a recent study, Kirillov et al. [9] proposed a new performance measure called Panoptic Quality for the panoptic segmentation task (e.g. instead of using $\text{Precision} \times \text{Recall}$ as AP), which can evaluate hard predictions. Therefore, the usage of AP on hard predictions does not fit into its ranking-based definition.
- *AP does not offer an optimal threshold for a detector.* Being defined as the area under the PR curve, any thresholding on detections decreases this area. Hence, performance with respect to AP increases, when the confidence score threshold approaches to 0 (i.e. the case of “no-thresholding”). As a result, it is not clear how the large number of object hypotheses can be reduced properly with AP when a visual detector is to be deployed in a practical application.
- *Using AP for classes with few examples is problematic owing to the interpolation of the PR curve (Section 3.1 for how PR curve is interpolated in AP computation).* Having few examples causes the recall axis to have a sparse set of values, and in this case interpolating the line segments spanning larger recall intervals will change the AUC more, which can especially have an effect for long-tail visual detection challenges such as LVIS [7] with a median of only 9 instances per class in the validation set.

We empirically analyse these limitations in Section 7.2.3.

4 PANOPTIC QUALITY

Following a similar methodology with how we analysed AP, this section provides an analysis for PQ.

4.1 Definition of PQ

The PQ measure is proposed to evaluate the performance of panoptic segmentation methods [9]. Given hard predictions (i.e. outputs without confidence scores), first, the detections are labelled as TP, FP and FN using an IoU-based criterion, and then the numbers of TPs (N_{TP}), FPs (N_{FP}), FNs (N_{FN}) and the localisation quality of TP detection masks in terms of IoU (i.e. $\text{IoU}(g_i, d_{g_i})$ is the IoU between the mask of the ground truth g_i and the mask of the associated detection, d_{g_i} , with g_i) are computed. Based on these quantities, PQ between a ground truth set \mathcal{G} and a detection set \mathcal{D} is defined as:

$$PQ(\mathcal{G}, \mathcal{D}) = \frac{1}{N_{TP} + \frac{1}{2}N_{FP} + \frac{1}{2}N_{FN}} \left(\sum_{i=1}^{N_{TP}} \text{IoU}(g_i, d_{g_i}) \right). \quad (1)$$

PQ is a “higher is better” measure with a range between 0 and 1, and includes the localisation quality of TPs, the number of FPs and the number of FNs. To provide more

TABLE 1: A comparison of LRP and PQ for the detectors (i.e. Detector 1 and Detector 2) in scenarios (a) and (b) in Figure 1 (Since PQ and LRP do not need confidence scores, scores are simply ignored for computing PQ and LRP in these scenarios.) PQ cannot identify the difference between these two scenarios, and yields exactly the same results for both of its components (i.e. SQ and RQ). With a component for each performance aspect, LRP can discriminate between these results using FP and FN components. While for PQ and components higher is better; for LRP, lower is better.

Scenario	PQ	SQ	RQ	Scenario	LRP	Loc	FP	FN
(a)	0.67	≈ 1	0.67	(a)	0.50	≈ 0	0.50	0.00
(b)	0.67	≈ 1	0.67	(b)	0.50	≈ 0	0.00	0.50

(a)
(b)

insight on the segmentation performance, PQ is split into two components: (i) Segmentation Quality (SQ), defined as the average IoU of the TPs, is a measure of the localisation performance; (ii) Recognition Quality (RQ) is a measure of classification performance defined as the F-measure. Using SQ and RQ, PQ can equally be expressed as: $PQ(\mathcal{G}, \mathcal{D}) = SQ(\mathcal{G}, \mathcal{D})RQ(\mathcal{G}, \mathcal{D})$.

4.2 An Analysis of PQ

In the following, we analyse PQ in terms of the same criteria that we used for AP:

Completeness. In contrast to AP, PQ precisely takes into account all performance aspects (i.e. FP rate, FN rate and localisation error - see “completeness” in Section 1.1) that are critical for visual detectors.

Interpretability. Another advantage of PQ compared to AP is that PQ is relatively more interpretable than AP owing to its SQ and RQ components. On the other hand, while Kirillov et al. [9] proposed using these components (i.e. SQ and RQ) to provide insight on the detection performance, RQ, the F-measure, is limited in terms of discriminating recall and precision performances (Table 1(a)). This is because each performance aspect does not have a separate component in PQ (i.e. the error types are not isolated [14]), but instead, both precision error and recall errors are combined into a single component, RQ. Therefore, overall, PQ is superior than AP in terms of interpretability, but having a component for each performance aspect is better to provide more useful insights.

Practicality. Here we discuss the following issues, which mostly arise since PQ is designed only for panoptic segmentation, and omit a discussion on its generalizability over all detection tasks:

- *Kirillov et al. [9] did not discuss how PQ can evaluate and threshold soft predictions (i.e. the outputs with confidence scores).* Kirillov et al. preferred hard predictions for panoptic segmentation to eliminate the inconsistency between machines and humans in terms of perceiving the objects. Accordingly, proposed for being limited to panoptic segmentation, PQ is designed to evaluate hard predictions, and its possible extensions

on soft predictions (and also other visual detection tasks) are not discussed and analysed by its authors.

- *PQ overpromotes classification performance compared to localisation performance inconsistently.* We observe the following for PQ: (i) Figure 3 illustrates how small shifts, induced by a TP, can cause large changes in PQ. Due to this promotion of a TP via a jump in the performance value, the effect of the localisation quality is decreased since the localisation quality can contribute between $PQ \in [0.50, 1.00]$ (Figure 3), (ii) While one can prefer classification error to have a larger effect on the overall performance, the formulation of PQ is inconsistent in terms of how localisation and classification performances are combined. In order to provide a comparative analysis with our performance metric, we discuss this inconsistency in Section 6. (iii) This inconsistent combination also makes PQ violate the triangle inequality property of metricity (see Appendix B for a proof).

5 LOCALISATION-RECALL-PRECISION (LRP) ERROR

In this section, we describe and analyse the LRP Error in Sections 5.1 and 5.2 respectively. Then, we present Optimal LRP (oLRP) as the extension of LRP for evaluating and thresholding soft-prediction-based visual object detectors (Section 5.3). We also discuss and present a guideline for other potential extensions of LRP Error (Section 5.4).

5.1 LRP: The Performance Metric

Definition: LRP is an error metric that considers both localisation and classification. To compute $LRP(\mathcal{G}, \mathcal{D})$ given a set of detections (\mathcal{D} - each $d_i \in \mathcal{D}$ is a tuple of class-label and location information), and a set of ground truth items (\mathcal{G}), first, the detections are assigned to ground truth items based on the matching criterion (e.g. IoU) defined for the corresponding visual detection task. Once the assignments are made, the following values are computed: (i) N_{TP} , the number of true positives; (ii) N_{FP} , the number of false positives; (iii) N_{FN} , the number of false negatives and (iv) the localisation qualities of TP detections, i.e. $lq(g_i, d_{g_i})$ for all d_{g_i} where d_{g_i} is a TP matching with ground truth g_i . Using these quantities, the LRP error is defined as:

$$LRP(\mathcal{G}, \mathcal{D}) := \frac{1}{Z} \left(\sum_{i=1}^{N_{TP}} \frac{1 - lq(g_i, d_{g_i})}{1 - \tau} + N_{FP} + N_{FN} \right), \quad (2)$$

where $Z = N_{TP} + N_{FP} + N_{FN}$ is the normalisation constant and τ is the TP validation threshold ($\tau = 0.50$ unless otherwise stated). Equation 2 can be interpreted as the “average matching error”, where the term in parentheses is the “total matching error”, and Z represents the “maximum possible value of the total matching error”. A TP contributes to the total matching error by its localization error normalized by $1 - \tau$ to ensure that the value is in interval $[0, 1]$ and LRP is a zeroth-order continuous function (Figure 3(c)). And, each FP or FN contributes to the total matching error by 1. Finally, normalisation by Z ensures $LRP(\mathcal{G}, \mathcal{D}) \in [0, 1]$. We prove

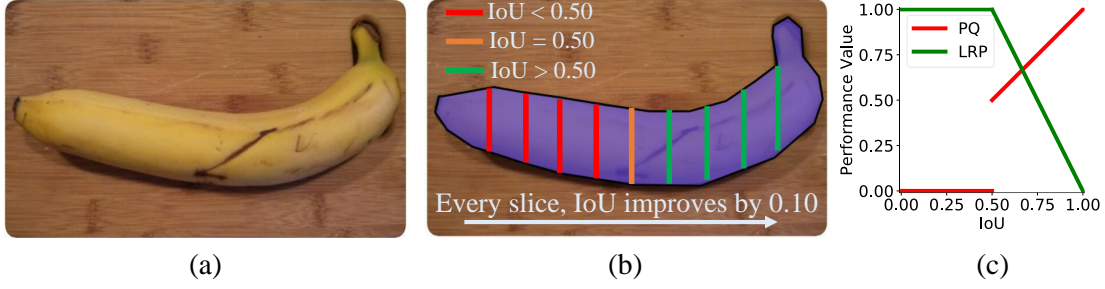


Fig. 3: An illustration that shows how a transition from a FP to TP is handled differently by PQ and LRP. (a) An example image from COCO [1]. (b) Segmentation masks for the ground truth with different IoU. The ground truth is split into 10 approximately equal slices. Orange line is the threshold where the detection is still a FP, hence a single pixel added makes the detection a TP. (c) How PQ and LRP changes for different IoU. While LRP is zeroth-order continuous, PQ is a discontinuous function and allows large jumps.

that LRP is a metric if $1 - \text{lq}(x_i, y_{x_i})$ is a metric (Appendix C).

Components: In order to provide additional information on the characteristics of the detector, we show that LRP can be equivalently defined in a weighted form as:

$$\text{LRP}(\mathcal{G}, \mathcal{D}) := \frac{1}{Z} (w_{\text{Loc}} \text{LRP}_{\text{Loc}}(\mathcal{G}, \mathcal{D}) + w_{\text{FP}} \text{LRP}_{\text{FP}}(\mathcal{G}, \mathcal{D}) + w_{\text{FN}} \text{LRP}_{\text{FN}}(\mathcal{G}, \mathcal{D})), \quad (3)$$

with the weights $w_{\text{Loc}} = \frac{N_{\text{TP}}}{1-\tau}$, $w_{\text{FP}} = |\mathcal{D}|$, and $w_{\text{FN}} = |\mathcal{G}|$ intuitively controlling the contributions of the terms as the upper bound of the contribution of a component (or performance aspect) to the “total matching error”. These weights ensure that each component corresponding to a performance aspect (Section 1.1) is easy to interpret, intuitively balances the components to yield Equation 2 and prevents the total error from being undefined whenever the denominator of a single component is 0. The first component, LRP_{Loc} , represents the localisation error of TPs as follows:

$$\text{LRP}_{\text{Loc}}(\mathcal{G}, \mathcal{D}) := \frac{1}{N_{\text{TP}}} \sum_{i=1}^{N_{\text{TP}}} (1 - \text{lq}(g_i, d_{g_i})). \quad (4)$$

The second component, LRP_{FP} , in Equation 3 measures the FP rate:

$$\text{LRP}_{\text{FP}}(\mathcal{G}, \mathcal{D}) := 1 - \text{Precision} = 1 - \frac{N_{\text{TP}}}{|\mathcal{D}|} = \frac{N_{\text{FP}}}{|\mathcal{D}|}, \quad (5)$$

and the FN rate is measured by LRP_{FN} :

$$\text{LRP}_{\text{FN}}(\mathcal{G}, \mathcal{D}) := 1 - \text{Recall} = 1 - \frac{N_{\text{TP}}}{|\mathcal{G}|} = \frac{N_{\text{FN}}}{|\mathcal{G}|}. \quad (6)$$

When necessary, the individual importance of localisation, FP, FN errors can be changed for different applications (Section 6 and Appendix D).

5.2 An Analysis of LRP

As we did for AP (Section 3.2) and PQ (Section 4.2), in the following we analyse LRP in terms of important features for a performance measure.

Completeness: Both definitions of LRP Error above (which are equivalent to each other) clearly take into account all performance aspects precisely, and ensure completeness (Section 1.1).

Interpretability: The ranges of total error and the components are $[0, 1]$, and a lower value implies better performance. LRP Error describes the “average matching error” (see Definition), and each component summarizes the error for a single performance aspect, thereby providing insights on the strengths and weaknesses of a detector. Therefore, LRP Error ensures interpretability (Section 1.1). In the extreme cases; $\text{LRP} = 0$ means that each ground truth item is detected with perfect localisation, and if $\text{LRP} = 1$, then no detection matches any ground truth (i.e., $|\mathcal{D}| = N_{\text{FP}}$).

Practicality: Since Equation 2 requires a thresholded detection set (i.e. does not require confidence scores), LRP can directly be employed to evaluate hard predictions, and can be computed exactly without requiring any interpolations or approximations. In the next section, we discuss how LRP can be extended to evaluate soft predictions using Optimal LRP (oLRP) and show that it can also be computed exactly. Also, in order to prevent the over-represented classes in the dataset to dominate the performance, similar to AP and PQ, LRP is computed class-wise and then these class-wise LRP errors are averaged to assign the LRP Error of a detector. One practical issue of LRP is that localisation and FP components are undefined when there is no detection, and the FN component is undefined when there is no ground truth. However, even if some components (not all) are undefined, the LRP Error is still defined (Equation 2). Namely, LRP is undefined only when the ground truth and detection sets are both empty (i.e., $N_{\text{TP}} + N_{\text{FP}} + N_{\text{FN}} = 0$), i.e., there is nothing to evaluate. When a component is undefined, we ignore the value while averaging it over classes.

5.3 Optimal LRP (oLRP): Evaluating and Thresholding Soft Predictions

Definition: Soft predictions (i.e. outputs with confidence scores) can be evaluated by, first, filtering the detections from a confidence score threshold and then, calculating LRP. We define Optimal LRP (oLRP) as the minimum achievable LRP error over the detection thresholds or equivalently, the

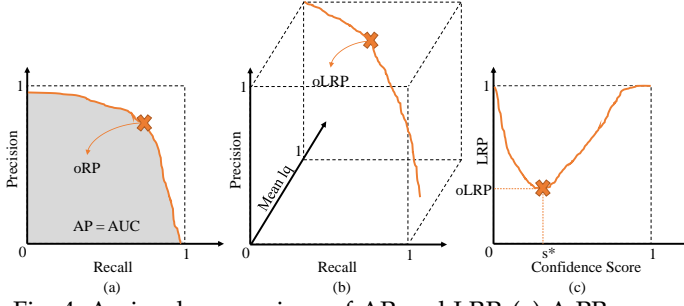


Fig. 4: A visual comparison of AP and LRP. (a) A PR curve. The cross marks a hypothetical optimal-recall-precision point (oRP) (e.g. the point where F1-measure is maximized). (b) A localisation, recall and precision curve, where “Mean lq” is the average localisation quality of TPs. Unlike any performance measure obtained via a PR curve (e.g. AP), LRP Error intuitively combines these performance aspects (Equation 2), and instead of area under the curve, uses the minimum of LRP values, defined as oLRP, as the performance metric. (c) An s-LRP curve to present the performance distribution of a detector for a class over confidence scores. Its minimum is oLRP.

confidence scores²:

$$\text{oLRP} := \min_{s \in \mathcal{S}} \text{LRP}(\mathcal{G}, \mathcal{D}_s), \quad (7)$$

where \mathcal{D}_s is the set of detections thresholded at confidence score s (i.e. those detections with larger confidence scores than s are kept, and others are discarded). Equation 7 implies searching over a set of confidence scores, \mathcal{S} , to find the best balance for competing precision, recall and localisation errors.

Components: The components of LRP for oLRP are coined as localisation@oLRP (oLRP_{Loc}), FP@oLRP (oLRP_{FP}), and FN@oLRP (oLRP_{FN}). oLRP_{Loc} describes the average localisation error of TPs, and oLRP_{FP} and oLRP_{FN} together indicate the point on the PR curve where optimal LRP is achieved. More specifically, one can infer the shape of the PR curve using the $(1 - \text{oLRP}_{FP}, 1 - \text{oLRP}_{FN})$ pair defining the optimal point on the PR curve.

Computation: Note that, theoretically, computing oLRP requires infinitely many thresholding operations since $\mathcal{S} = [0, 1]$. However, given that \mathcal{S} is discretised by the scores of the detections, in order to compute oLRP exactly, it is sufficient to threshold the detection set only at the confidence scores of the detections. More formally, for two successive detections d_i and d_j (in terms of confidence scores) with confidence scores s_i and s_j where $s_i > s_j$, $\text{LRP}(\mathcal{G}, \mathcal{D}_s) = \text{LRP}(\mathcal{G}, \mathcal{D}_{s_j})$ if $s_j \leq s < s_i$. Then, oLRP for a class can be computed **exactly** by minimizing the finite LRP values on the detections, and one can average oLRP and its components over classes to obtain the performance of the detector.

oLRP as a Thresholder: Conventionally, visual object detectors yield numerous detections [25], [30], [31], most of which

have smaller confidence scores. In order to deploy an object detector for a certain problem, the detections with “smaller” confidence scores need to be discarded to provide a clear output from the visual detector (i.e. model selection). While it is common to use a single class-independent threshold for the detector (e.g., Association-LSTM [28] uses SSD [24] detections for all classes with confidence score above 0.80), we show in Section 7.4 that (i) the performances of the detectors are sensitive to thresholding, and (ii) the thresholding needs to be handled in a class-specific manner. Note that balancing the competing performance aspects in an optimal manner, oLRP satisfies these requirements. In particular, we define the confidence score threshold corresponding to the oLRP Error as the “LRP-Optimal Threshold” (s^* —see Figure 4). Different from the common approach, (i) s^* is a class-specific optimal threshold, and (ii) s^* considers all performance aspects of visual detection tasks (Figure 4). See Appendices D and H for a further discussion on thresholding object detectors.

5.4 Potential Extensions of LRP

This section discusses potential extensions of LRP Error in three levels:

Extension to Other Localisation Quality Functions:

Any localisation function that satisfies the following two constraints can be used within LRP: (i) $\text{lq}(\cdot, \cdot)$ should be a higher-better function, and (ii) $\text{lq}(\cdot, \cdot) \in [0, 1]$. In addition, choosing a $\text{lq}(\cdot, \cdot)$ such that $1 - \text{lq}(\cdot, \cdot)$ is a metric, guarantees the metricity of LRP Error. In case constraint (ii) is violated by a prospective $\text{lq}(\cdot, \cdot)$, then one can normalize the range of the function (and also TP validation threshold, τ) to satisfy this constraint. For example, as a recently proposed IoU variant to measure the spatial similarity between two bounding boxes, Generalized IoU (GIoU) [22] has a range of $[-1, 1]$. In this case, choosing $\text{lq}(\cdot, \cdot) = \text{GIoU}(\cdot, \cdot)/2 + 0.50$ will allow the use of GIoU within LRP.

Extension to New Detection Tasks: While adopting for new detection tasks, one should only consider the localisation quality function (see above). Following this, LRP can easily be adapted to new or existing detection tasks such as 3D object detection and rotated object detection.

Extension to Other Fields: LRP can be extended for any problem with the following two properties in terms of evaluation: (i) the similarity between a TP and its matched ground truth can be measured by using a similarity function (preferably a metric to ensure the metricity of LRP), and (ii) at least one of the classification errors (i.e. FP error or FN error) matters for performance. Then, to use LRP Error, it is sufficient to ensure the similarity function satisfy the constraints for $\text{lq}(\cdot, \cdot)$ (see extension to other localisation quality functions). If either FP or FN error is not included in the task, then one can set the number of errors originating from the missing component (i.e. N_{FP} or N_{FN}) to 0 and proceed with Equation 2.

6 A COMPARISON OF LRP WITH AP AND PQ

To better understand the behaviours of the studied performance measures (AP, PQ and LRP) and make comparisons, we plot them in the three dimensional space of mean

2. Another way to evaluate soft predictions is the Average LRP (aLRP), the average of the LRP Errors over the confidence scores. While in a recent study [20], we showed that aLRP can be used as a loss function, we discuss in Appendix E why we preferred oLRP over aLRP as a performance measure.

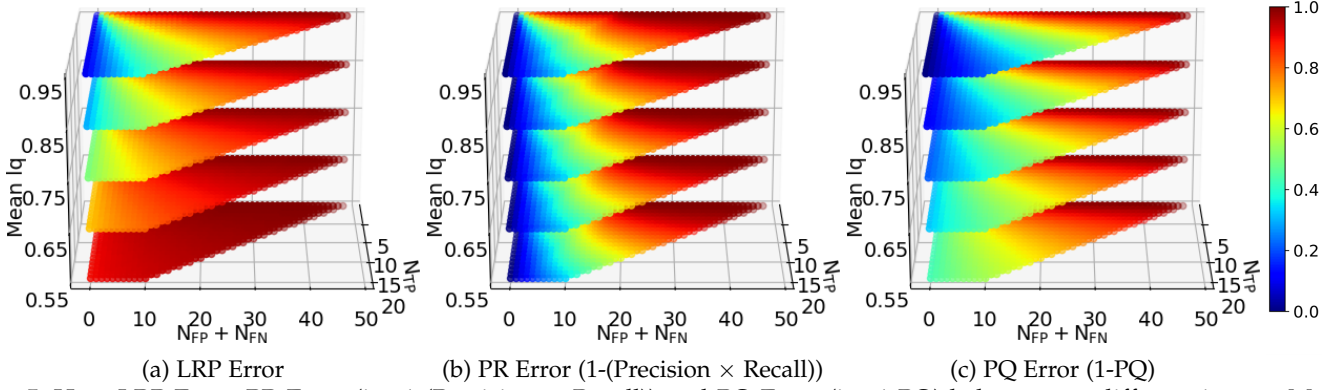


Fig. 5: How LRP Error, PR Error (i.e. $1 - (\text{Precision} \times \text{Recall})$) and PQ Error (i.e. $1 - \text{PQ}$) behave over different inputs. Mean lq is the average localisation qualities of TPs. PR Error ignores localisation and PQ overpromotes classification compared to localisation. The space is uniformly discretized and error combinations of up to 20 ground truths and 50 detections are depicted.

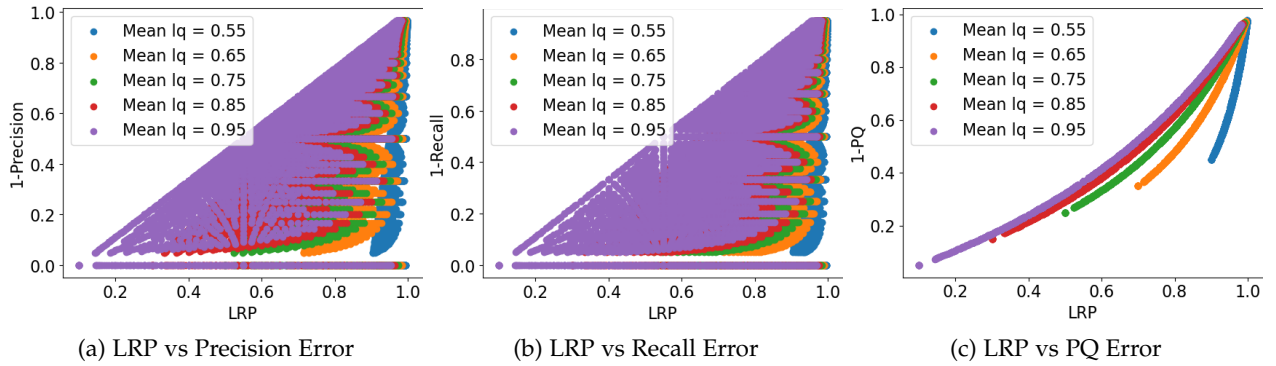


Fig. 6: The relation of LRP with (a) precision error (1-precision), (b) recall error (1-recall) and (c) PQ error (1-PQ) using the examples from Figure 5. LRP Error is an upper bound for precision, recall and PQ errors. Since LRP includes recall (precision) and localisation in addition to precision (recall) error, the correlation between precision (recall) error and LRP is not strong. On the other hand, with similar definitions LRP and PQ evaluate similarly, but still their difference increases when Mean lq decreases since PQ suppresses the effect of localisation by promoting classification more.

localisation quality, N_{TP} and $N_{FP} + N_{FN}$ (Figure 5). To facilitate comparison, we represent AP and PQ by their “error” versions, that is, for AP, we use “PR Error” which is $1 - \text{Precision} \times \text{Recall}$; and for PQ, we use “PQ Error” which is $1 - \text{PQ}$. Firstly, note that, PR Error stays the same as you move parallel to the “Mean lq” axis as expected (Figure 5(b)). This is because PR Error, hence AP, uses the localisation quality just to validate TPs, and it does not take into account the quality above the TP-validation threshold. Secondly, PQ Error is lower than LRP Error at low “Mean lq”, e.g. 0.55 and 0.65, low $N_{FP} + N_{FN}$ and large N_{TP} (Figure 5(a) and (c)). This is due to the fact that PQ Error prefers to emphasize classification over localisation (as discussed in Section 4). On the other hand, as hypothesized in Section 4, the way how PQ overpromotes classification is inconsistent. To show this, we first demonstrate that LRP and PQ Errors have quite similar definitions. PQ Error can be written as (see Appendix F for the derivation):

$$1 - \text{PQ} = \frac{1}{\hat{Z}} \left(\sum_{i=1}^{N_{TP}} \frac{1 - \text{lq}(g_i, d_{g_i})}{1 - 0.50} + N_{FP} + N_{FN} \right), \quad (8)$$

where $\hat{Z} = 2N_{TP} + N_{FP} + N_{FN}$. Note that setting $\tau = 0.50$ and removing the coefficient of N_{TP} in \hat{Z} (in red) results

in $1 - \text{PQ} = \text{LRP}$ (Equation 2), which implies very similar definitions for PQ and LRP Errors (and note that LRP was proposed before PQ): Equation 8 presents that (i) the “total matching error” of PQ and LRP Errors are equal (Section 5.1 for total matching error), and (ii) PQ Error prefers doubling N_{TP} in the normalisation constant instead of normalizing the total matching error directly by its maximum value (i.e. $N_{TP} + N_{FP} + N_{FN}$) as done by LRP. Therefore, keeping the total matching error the same, the normalisation constant of PQ Error grows inconsistently. In other words, the rates of the change of the total matching error and its maximum possible value are different. As suggested in our previous work [8], a consistent prioritization of a performance aspect can be achieved by including its coefficient to both total matching error (i.e. nominator) and its maximum value (i.e. denominator) as follows:

$$\frac{1}{Z} \left(\sum_{i=1}^{N_{TP}} \alpha_{TP} \frac{1 - \text{lq}(g_i, d_{g_i})}{1 - \tau} + \alpha_{FP} N_{FP} + \alpha_{FN} N_{FN} \right) \quad (9)$$

where $Z = \alpha_{TP} N_{TP} + \alpha_{FP} N_{FP} + \alpha_{FN} N_{FN}$. Following the interpretation of LRP (Section 5.1), these coefficients imply duplicating each error source, hence the consistency between the total matching error and its maximum value is preserved (see Appendix D for more discussion).

TABLE 2: Comparison of AP, PQ and LRP in terms of desired properties. While LRP ensures all three, AP turns out to be limited in these properties.

Measure	Completeness	Interpretability	Practicality
AP	✗	✗	<ul style="list-style-type: none"> • limited to soft predictions • does not offer an optimal confidence score threshold • uses interpolation
PQ	✓	✓	<ul style="list-style-type: none"> • limited to panoptic segmentation • overpromotes the classification performance inconsistently
LRP	✓	✓	✓

In Figure 6, we present the relationship of LRP with precision, recall and PQ Errors, which show that **LRP is an upper bound for all other error measures**. As a result, improving LRP can be considered a more challenging task than improving the other two error measures.

The comparison of LRP with AP and PQ in terms of the important features (Section 1.1) of a performance measure for visual object detectors is summarized in Table 2. Please refer to Sections 3, 4 and 5 for further discussion.

7 EXPERIMENTAL EVALUATION

In this section, we first present the usage and discriminative abilities of the LRP Error on visual detection tasks in comparison to AP variants (Section 7.2) and PQ (Section 7.3). Then, we show that the performances of object detectors are sensitive to thresholding (Section 7.4) and provide a use-case of LRP-Optimal Thresholds (Appendix H.1). Also we analyse the additional overhead of LRP computation and the behaviour of LRP under different TP validation thresholds in Appendix H. We would like to note that our main motivation is to present insights on LRP and represent its evaluation capabilities rather than choosing which detection method is better.

7.1 Evaluated Models, Datasets and Performance Measures

Evaluated Models: We use LRP to evaluate 35 state of the art (SOTA) methods (i.e. 32 methods to evaluate soft predictions in Section 7.2 and 3 methods to evaluate hard predictions in Section 7.3) obtained from three widely-used repositories: mmdetection [17], detectron [32] and detectron2 [11]³. We provide the corresponding repository of each model in Appendix G to facilitate the usage and reproduction of our results. We do not retrain the models but use the already trained instances provided in their repositories. We use R50, R101 and X101 as abbreviations for ResNet-50, ResNet-101 and ResNext-101 backbones, respectively.

Datasets: We use the COCO [1] dataset, one of the most widely used detection datasets which provides ground-truth annotations for 80 object classes, for all four visual detection tasks that we are interested in. The training and testing sets of the used models are *COCO 2017 train* (~118k images) and *COCO 2017 val* (5k images). Note that the panoptic segmentation task additionally requires the annotation of the ‘stuff’ classes, which are not included in

the 80 object classes. Hence, for panoptic segmentation, we follow the configuration of detectron2, where 53 additional stuff classes are acquired from the COCO-stuff dataset [33].

Performance Measures: On tasks with hard-predictions (i.e. panoptic segmentation), we compare LRP with PQ. On the remaining three tasks, namely object detection, keypoint detection and instance segmentation, all of which are soft-prediction tasks, we compare LRP with AP. Since AP does not explicitly have performance components, we include the following measures to facilitate comparison:

- 1) AP_{75} , in which τ , the TP validation threshold, is 0.75. AP_{75} is a popular measure to represent the localisation accuracy of a method.
- 2) AP_{50} , to represent the classification component.
- 3) AR_r^C (Average Recall) where r is the number of top-scoring detections to include in the computation of AR. Note that AR_r^C is also COCO-style (i.e. averaged over 10 τ thresholds - see the definition of COCO-style AP, denoted by AP^C , in Section 3).

7.2 Evaluating Soft Predictions on Object Detection, Keypoint Detection and Instance Segmentation Tasks

This section compares oLRP with AP&AR variants for soft predictions and shows that oLRP is more discriminative and interpretable. The structure of this section is based on the limitations (Section 1.2) and analysis of AP (Section 3.2) in terms of the important features (Section 1.1). While demonstrating these limitations and comparing with oLRP, we use both detector-level results (Table 3) and class-level results (Table 4) of the SOTA methods. For the detector-level performance comparison, we present the results of 32 SOTA visual detectors on all three visual detection tasks. In order to provide insight on oLRP and its components and illustrate its usage at the class level, we select a subset of six object detectors by ensuring diversity (e.g. different backbones, one- and two-stage detectors, different assignment and sampling strategies etc.) and evaluate their performance on “person” and “broccoli” classes.

7.2.1 Analysis with respect to Completeness

AP loosely includes the localisation quality (Section 3.2). Here we discuss the benefits of directly using the localisation quality as an input to the performance measure.

Firstly, to see how AP_{50} fails to include localisation quality precisely, we consider the following three detectors with equal AP_{50} (63.7%) in Table 3: Faster R-CNN (X101-12), Libra R-CNN and Guided Anchoring. oLRP and AP^C ,

3. One exception is aLRP Loss, for which we use our own implementation.

TABLE 3: AP and oLRP performances of several methods for soft-prediction tasks (i.e. object detection, keypoint detection and instance segmentation) on COCO 2017 val. For AR_r^C , $r = 100$ for object detection and instance segmentation, while it is 20 for keypoint detection.

Method	Backbone	Epoch	AP & AR				oLRP & Components			
			AP ^C ↑	AP ₅₀ ↑	AP ₇₅ ↑	AR _r ^C ↑	oLRP ↓	oLRP _{Loc} ↓	oLRP _{FP} ↓	oLRP _{FN} ↓
Object Detection:										
<i>One Stage Methods:</i>										
SSD-300 [24]	VGG16	120	25.6	43.8	26.3	37.5	78.4	20.6	37.1	57.9
SSD-512 [24]	VGG16	120	29.4	49.3	31.0	42.5	75.4	19.7	32.8	53.6
RetinaNet [30]	R50	12	35.7	54.7	38.5	52.0	71.0	17.0	29.1	50.0
RetinaNet [30]	R50	24	35.7	54.9	38.2	51.4	70.6	17.1	28.4	49.6
RetinaNet [30]	X101	24	39.2	59.2	41.8	53.5	67.5	16.1	24.5	46.3
ATSS [34]	R50	12	39.4	57.6	42.8	58.3	68.6	15.4	30.3	46.6
RetinaNet [30]	X101	12	39.8	59.5	43.0	54.8	67.6	16.1	25.3	46.2
NAS-FPN [35]	R50	50	40.5	58.4	43.1	55.6	66.7	14.8	26.6	46.3
GHM [36]	X101	12	41.4	60.9	44.2	57.7	66.3	15.6	27.1	44.2
FreeAnchor [37]	X101	12	41.9	61.0	45.0	58.6	66.0	15.2	26.4	44.5
FCOS [31]	X101	24	42.5	62.1	45.7	58.2	64.4	14.9	25.4	41.9
RPDet [38]	X101	24	44.2	65.5	47.8	58.7	63.3	15.4	23.4	39.5
aLRP Loss [20]	X101	100	45.4	66.6	48.0	60.3	62.5	15.1	23.2	39.5
<i>Two Stage Methods:</i>										
Faster R-CNN [25]	R50	24	37.9	59.3	41.1	51.0	68.8	17.4	25.7	45.4
Faster R-CNN [25]	R101	12	39.4	61.2	43.4	52.6	67.6	17.2	24.2	44.3
Faster R-CNN [25]	R101	24	39.8	61.3	43.3	52.5	67.3	16.8	25.5	43.4
Faster R-CNN [25]	X101	12	41.3	63.7	44.7	54.6	66.2	17.1	24.9	41.5
Libra R-CNN [39]	X101	12	42.7	63.7	46.9	56.0	65.1	15.8	24.3	41.6
Grid R-CNN [40]	X101	24	43.0	61.6	46.7	56.7	64.2	14.4	24.7	42.3
Guided Anchoring [41]	X101	12	43.9	63.7	48.3	59.9	64.4	14.8	25.6	41.8
Cascade R-CNN [21]	X101	20	44.5	63.2	48.5	56.9	63.3	14.3	25.4	41.0
Cascade R-CNN [21]	X101	12	44.7	63.6	48.9	57.4	63.2	14.4	23.9	40.9
Keypoint Detection:										
Keypoint R-CNN	R50	12	64.0	86.4	69.3	71.0	44.8	12.8	10.8	18.6
Keypoint R-CNN	R50	37	65.5	87.2	71.1	72.4	43.0	12.3	10.4	17.3
Keypoint R-CNN	R101	37	66.1	87.4	72.0	73.1	42.0	11.9	9.0	17.8
Keypoint R-CNN	X101	37	66.0	87.3	72.2	73.2	41.9	11.7	8.8	18.1
Instance Segmentation:										
Mask R-CNN [42]	R50	24	35.4	56.4	37.9	48.1	70.7	18.5	28.5	47.0
Mask R-CNN [42]	R101	24	36.6	57.9	39.1	48.8	69.4	18.2	25.9	46.3
Mask R-CNN [42]	X101	12	38.4	60.6	41.3	50.3	67.8	18.3	24.9	43.5
Cascade Mask R-CNN [21]	X101	20	39.5	61.3	42.5	50.5	66.8	18.0	24.3	42.1
Mask Scoring R-CNN [43]	X101	12	39.5	60.5	42.6	50.1	67.5	17.9	24.5	43.3
Hybrid Task Cascade [44]	X101	20	43.8	66.8	47.1	57.4	63.6	17.0	23.4	37.9

TABLE 4: AP and oLRP performances of several object detectors for two selected classes, namely, “person” and “broccoli”, on COCO 2017 val. The horizontal line splits one- and two-stage object detectors.

Class	Method	Backbone	Epoch ⁴	AP & AR				oLRP & Components			
				$AP^C \uparrow$	$AP_{50} \uparrow$	$AP_{75} \uparrow$	$AR_{100}^C \uparrow$	$oLRP \downarrow$	$oLRP_{Loc} \downarrow$	$oLRP_{FP} \downarrow$	$oLRP_{FN} \downarrow$
Person	ATSS [34]	R50	12	54.7	81.4	59.3	64.8	55.6	15.4	14.8	27.8
	FCOS [31]	X101	24	55.3	82.4	59.1	64.2	53.5	15.0	13.0	26.2
	RetinaNet [30]	X101	12	51.1	79.0	54.6	60.1	58.3	16.3	14.1	31.0
	aLRP Loss [20]	X101	100	57.7	84.3	61.7	66.6	52.1	14.5	11.2	26.3
	Faster R-CNN [25]	R101	24	53.8	82.8	57.9	61.2	55.3	16.3	11.1	27.7
	Cascade R-CNN [21]	X101	12	57.8	83.4	62.7	65.2	52.1	14.6	13.5	24.5
	ATSS [34]	R50	12	24.1	43.3	24.0	55.0	81.6	20.1	53.2	52.9
Broccoli	FCOS [31]	X101	24	21.9	41.5	21.6	48.4	82.4	21.4	45.1	58.7
	RetinaNet [30]	X101	12	22.1	44.4	19.7	49.3	81.3	21.8	41.3	56.7
	aLRP Loss [20]	X101	100	24.3	45.5	23.5	51.7	80.2	21.2	45.7	51.6
	Faster R-CNN [25]	R101	24	22.0	43.6	19.3	43.8	81.2	22.7	49.2	48.4
	Cascade R-CNN [21]	X101	12	24.3	43.9	25.5	47.2	80.2	20.1	51.8	48.7

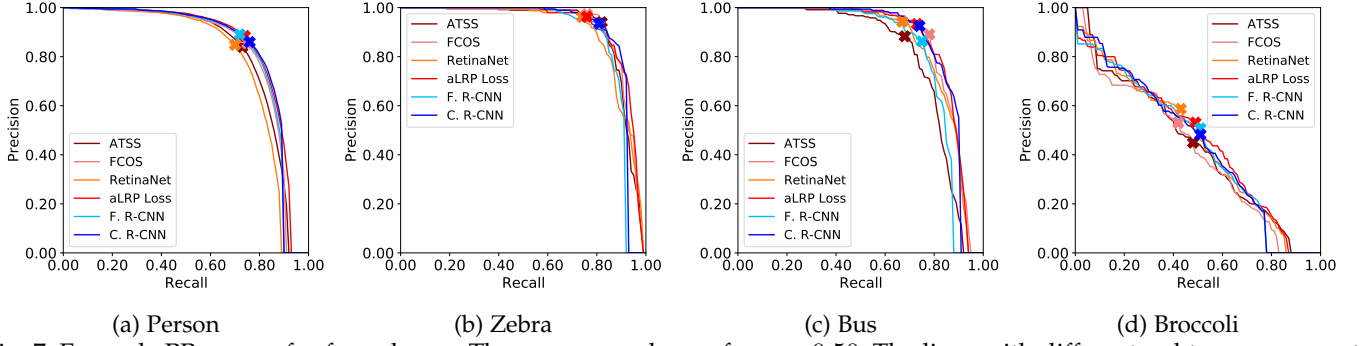


Fig. 7: Example PR curves for four classes. The curves are drawn for $\tau = 0.50$. The lines with different red tones represent one-stage detectors whereas those with blue tones correspond to two-stage detectors. While AP_{50} considers the area under the curve, LRP combines localisation, recall and precision errors, and hence optimal LRP points, marked with crosses, are found in the top right part of the curves. Detailed results of “person” and “broccoli” can be found in Table 4. F. R-CNN: Faster R-CNN, C. R-CNN: Cascade R-CNN

which take into account the localisation quality, rank these three detectors differently (Table 3). Therefore, AP_{50} should not be selected as the single performance measure for benchmarking since it neglects localisation.

To illustrate the drawback of AP^C or AP_{75} in terms of localisation, note that while neither AP^C nor AP_{75} assigns the largest performance value to NAS-FPN among one-stage object detectors, this detector has the least average localisation error ($oLRP_{Loc}$ - see Table 3): e.g. GHM outperforms NAS-FPN by 1.1% in terms of AP_{75} , while its average localisation performance is 0.8% lower than NAS-FPN. Therefore, AP^C and AP_{75} , too, may fail to appropriately compare methods in terms of localisation quality.

Using $oLRP$ is easier and more intuitive than using the AP variants mentioned above: (i) Unlike these AP variants, $oLRP$ Error consistently and precisely (not loosely) combines localisation, FP and FN errors, and in this case, the performance gap between NAS-FPN and GHM reduces to 0.4% in terms of $oLRP$ (i.e. while GHM outperforms NAS-FPN by 1.1% with respect to AP^C) thanks to the localisation performance of NAS-FPN. (ii) Different from all AP variants, $oLRP_{Loc}$ quantifies the localisation error precisely and allows direct comparison among methods, classes, etc.: e.g. NAS-FPN outperforms GHM by 0.8% in terms of $oLRP_{Loc}$. (iii) One can easily interpret $oLRP_{Loc}$ both at the class- and detector-level: for example, for ATSS, IoU is $1 - 0.154 = 0.846$ and $1 - 0.201 = 0.799$ for the “person” and “broccoli” classes respectively (Table 4).

Finally, being an interpretable localisation measure, $oLRP_{Loc}$ can facilitate analysis of detectors. For example, in Table 3, we can easily notice for $oLRP_{Loc}$ that instance segmentation task has room for improvement in terms of localisation compared to other tasks. In particular, even the best performing instance segmentation method, Hybrid Task Cascade (HTC), yields 17.0% $oLRP_{Loc}$ error which corresponds to a mediocre localisation error for the object detectors and keypoint detectors, typically achieving 14.3% and 11.7% $oLRP_{Loc}$ errors, respectively. With this 17.0%, HTC has a similar localisation performance with RetinaNet (R50-24) in terms of $oLRP_{Loc}$. Again, HTC outperforms RetinaNet (R50-24) by around 10% AP_{75} , suggesting that the same deduction cannot be obtained by AP_{75} .

7.2.2 Analysis with respect to Interpretability

This section presents insights about the interpretability of $oLRP$ Error compared to AP (see Section 3.2 for a discussion on the limited interpretability of AP).

While any AP variant does not provide insight on the performance of an object detector, the components of $oLRP$ provide useful insight on the performance. To illustrate, we compare two object detectors with equal AP^C , ATSS and Faster R-CNN (R101-12) (see in Table 3 that both have 39.4% AP^C), using AP & AR based measures and $oLRP$ & components as follows:

- Faster R-CNN (R101-12) outperforms ATSS by 3.6% and 0.6% in terms of both AP_{50} and AP_{75} and ATSS outperforms Faster R-CNN (R101-12) by around 6% with respect to AR_{100}^C . Note that a clear conclusion (i.e. quantifying which detector is better on which performance aspect) is not possible with these AP & AR based measures since AP_{50} and AP_{75} are combinations of precision & recall and AR_{100}^C a combination of recall & localisation quality.
- As for $oLRP$, Faster R-CNN (R101-12) outperforms ATSS by 6.1% and 2.3% in terms of FP and FN Errors respectively, and ATSS has 1.8% better localisation performance than Faster R-CNN (R101-12). Since each component corresponds to one performance aspect, one can easily deduce that while Faster R-CNN has better classification performance (wrt. both precision and recall), ATSS localises objects better. Overall, combining these components consistently, in this case, $oLRP$ prefers Faster R-CNN (R101-12) over ATSS by 1.1% while they have the same AP^C .

In addition, $oLRP_{FP}$ and $oLRP_{FN}$ provide insight on the structure of the PR curve by representing the point on the PR curve where the minimal LRP is achieved. To illustrate, for all methods, the “person” class has lower FP & FN error values than the “broccoli” class, implying the $oLRP$ point of the “person” PR curve to be closer to the top-right corner. To see this, note that Faster R-CNN has 11.1% and 27.7% FP and FN error values, respectively for the “person” class (Table 4). Thus, without looking at the curve, one may conclude that the $oLRP$ point resides at $1 - 0.111 = 0.889$ precision and $1 - 0.277 = 0.723$ recall. For the “broccoli”

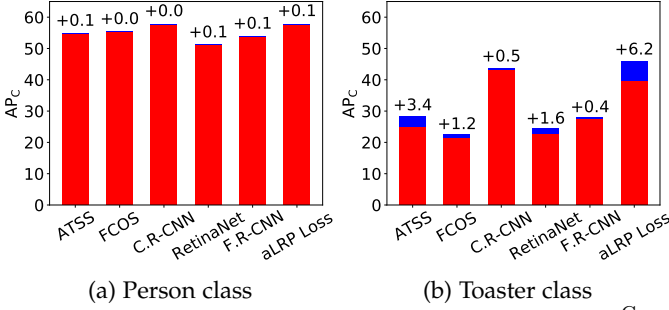


Fig. 8: The effect of interpolating the PR curve on AP^C on (a) the “person” class, the class with the most number of examples, (b) the “toaster” class, the class with the least number of examples. Red: AP without interpolation. Blue: Additional AP^C after interpolation. The numbers on the bars indicate this additional AP^C points due to interpolation. While the effect of interpolation is negligible for the “person” class, there is a significant effect of interpolation (i.e. 2.2% AP^C on average, up to 6.2%) on the performance of the toaster class (i.e. the class with the minimum number of examples) for all the detectors. C.R-CNN: Cascade R-CNN, F.R-CNN: Faster R-CNN.

curve, the oLRP point is achieved at $1 - 0.492 = 0.508$ and $1 - 0.484 = 0.516$ as precision and recall, respectively. Unlike the “person” class, these values suggest that the optimal point of the “broccoli” class is around the center of the PR range (cf. Figure 7(a) and (d)). Hence, oLRP_{FP} and oLRP_{FN} are also easily interpretable and in such a way, exhaustive examination of PR curves can be alleviated.

Similar to oLRP_{loc}, oLRP_{FP} and oLRP_{FN} facilitate analysis as well, which is not straightforward by using AP&AR based measures. Suppose that we want to compare precision and recall performances of the visual object detectors. Comparing oLRP_{FP} and oLRP_{FN}, it is obvious that current object detectors have significantly lower precision error than recall error (i.e. oLRP_{FP} - oLRP_{FN} is around 15% to 20 % for object detection and instance segmentation, 7% to 8 % for keypoint detection - see Table 3). Given AP&AR based measures, one alternative can be to compare AP_{50} with AR_{100}^C , which is again hampered by the loose and indirect combination of the performance aspects: Note that while oLRP_{FP} and oLRP_{FN}, isolating errors with respect to performance aspects, assign significantly more recall error than precision error for ATSS (oLRP_{FN} - oLRP_{FP} = 16.5% - see Table 3), AP- and AR- based performance measures favor recall performance over precision performance ($AR_{100}^C > AP_{50}$). Therefore, indirect contribution of the performance aspects makes the analysis more difficult for AP- and AR-based measures, while oLRP and components are easier to interpret and compare.

7.2.3 Analysis with respect to Practicality

This section presents how LRP variants can handle the practical disadvantages of AP (see Section 3.2 for a discussion why AP is limited in these practical issues).

Evaluating Hard Predictions: We discuss how LRP evaluates hard predictions in Section 7.3.

Thresholding Visual Object Detectors: We discuss our class-specific thresholding approach using LRP-Optimal

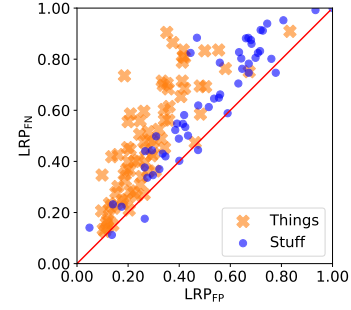


Fig. 9: Class-level LRP_{FP} vs. LRP_{FN} comparison. Overall, there is a tendency of larger LRP_{FN} error than LRP_{FP} error. This is more obvious for things classes. It is not possible to make the same observation using RQ.

thresholds in Section 7.4.

The Effect of Interpolation: In order to present the effect of interpolation on classes with relatively fewer number of examples, we compute AP^C of the same six detectors from class-level comparison table (Table 4) with and without interpolation on two classes: (i) the “person” class as the class with maximum number examples in COCO val 2017 (i.e. 21554 examples), and (ii) the “toaster” class, the class with the minimum number of examples (i.e. 17 examples). The AP^C difference is presented in Figure 8, in which the significant effect of interpolation on the class with the less number of examples is clearly observed: (i) While the average AP^C difference over detectors between with and without interpolation is almost negligible for person class (i.e. less than 0.1% AP^C), it is around 35× more for the toaster class (2.2% AP^C), (ii) There is even 6.2% jump for the aLRP Loss after interpolation. Note that this corresponds to around a superficial 20% relative performance improvement (from 33.4% to 39.6%) in terms of AP^C . Therefore, while the AP variants are sensitive to interpolation especially for the rare classes in the dataset, oLRP does not employ interpolation. This issue of AP should especially be taken care of for visual detection datasets with rare classes such as LVIS [7]. Note that unlike AP, oLRP computation is exact (Section 5.3).

7.3 Evaluating Hard Predictions on Panoptic Segmentation Task

In this section, we apply LRP Error to panoptic segmentation task to present its ability to evaluate hard predictions and also compare LRP with PQ. In particular, we evaluate three different variants of Panoptic FPN [45] using both LRP and PQ, and present the results in Table 5 in three groups: (i) “All” includes all 133 classes, (ii) “Things” includes 80 object classes, and (iii) “Stuff” includes the remaining 53 classes, normally counted as background by other detection tasks. Similar to oLRP, we follow our analysis on PQ (Section 4.2) except the superiority of LRP on evaluating and thresholding soft predictions, which we discuss in Sections 7.2 and 7.4 respectively.

7.3.1 Analysis with respect to Interpretability

The RQ component of PQ, the F-measure, does not provide discriminative information on precision and recall errors.

TABLE 5: Detector-level performance results of panoptic segmentation methods as hard predictions. For each method, besides an overall average in All classes, we provide the performance of things and stuff as well.

Method	Backbone	Epoch	Type	PQ & Components			LRP & Components			
				PQ \uparrow	SQ \uparrow	RQ \uparrow	LRP \downarrow	LRP _{Loc} \downarrow	LRP _{FP} \downarrow	LRP _{FN} \downarrow
Panoptic FPN [45]	R50	12	All	39.4	77.8	48.3	77.5	22.2	40.2	57.2
			Things	45.9	80.9	55.3	72.7	18.1	29.4	51.7
			Stuff	29.6	73.3	37.7	84.6	25.3	54.3	65.5
Panoptic FPN [45]	R50	37	All	41.5	79.1	50.5	75.9	20.3	38.6	55.2
			Things	48.3	82.2	57.9	70.8	17.8	29.3	49.1
			Stuff	31.2	74.4	39.4	83.5	24.2	52.6	64.4
Panoptic FPN [45]	R101	37	All	43.0	80.0	52.1	74.6	19.4	37.0	53.6
			Things	49.7	82.9	59.2	69.4	17.1	28.4	47.6
			Stuff	32.9	75.6	41.3	82.3	22.9	50.2	62.7

On the other hand, LRP presents more insight on these errors with its FP and FN components. To illustrate, all Panoptic FPN variants suffer from the recall error more than the precision error, and this is more obvious for “things” classes: (i) Table 5 shows that $LRP_{FN} > LRP_{FP}$ for all methods in class groups. (ii) While the gap between LRP_{FP} and LRP_{FN} for “stuff” classes is around 10%, it is around 20% for “things” classes for all detectors. (iii) Finally, the same difference between “things” and “stuff” classes can easily be observed at the class-level in Figure 9 where the error is skewed towards LRP_{FN} . Therefore, we argue that LRP FP and FN components present more insight than RQ.

7.3.2 Analysis with respect to Practicality

Since the definitions of LRP and PQ are similar (Equation 8), LRP and PQ generally rank the detectors and classes similarly. However, we observed certain differences owing to the over-promotion of TPs by PQ with its discontinuous nature: (i) We observed that 205 pair of classes for which the evaluation results of LRP and PQ conflict (i.e. $(PQ_i < PQ_j)$ and $(LRP_j > LRP_i)$ where the subscript represents the class label). As expected (see also Figure 5(a,c) and Figure 6(c)), PQ favors classes with more TPs compared to LRP, and LRP favors the classes with better localisation performance. (ii) In some cases, the difference between the results of AP and PQ (i.e. $(PQ_i - PQ_j) - (LRP_j - LRP_i)$) can be large. For example, while the “bicycle” and “orange” classes have 40.6% and 34.1% PQ respectively (i.e. “bicycle” outperforms by 6.5), their LRP values are 82.4% and 81.5% (i.e. “orange” outperforms by 0.9%). Overall these imply a 7.4% difference between AP and LRP. The over-promotion of TPs by PQ can also be observed by examining its components: While the RQ of “bicycle” and “orange” are 55.9% and 38.4% respectively (i.e. “bicycle” outperforms by 17.5%), SQ are 72.7% and 88.9% (i.e. “orange” outperforms by 16.2%). These results suggest that while “bicycle” can be classified better than “orange”, the localisation performance of “bicycle” is poorer. As a result, while LRP results are similar, PQ promotes the class with better classification (i.e. “bicycle”) by 6.5% and assigns a lower priority to localisation.

7.4 Thresholding Visual Object Detectors

In this section, we show that (i) the performances of visual detectors is sensitive to thresholding, (ii) the thresholds need

to be set in a class-specific manner and (iii) LRP-Optimal thresholds can be used to alleviate this sensitivity.

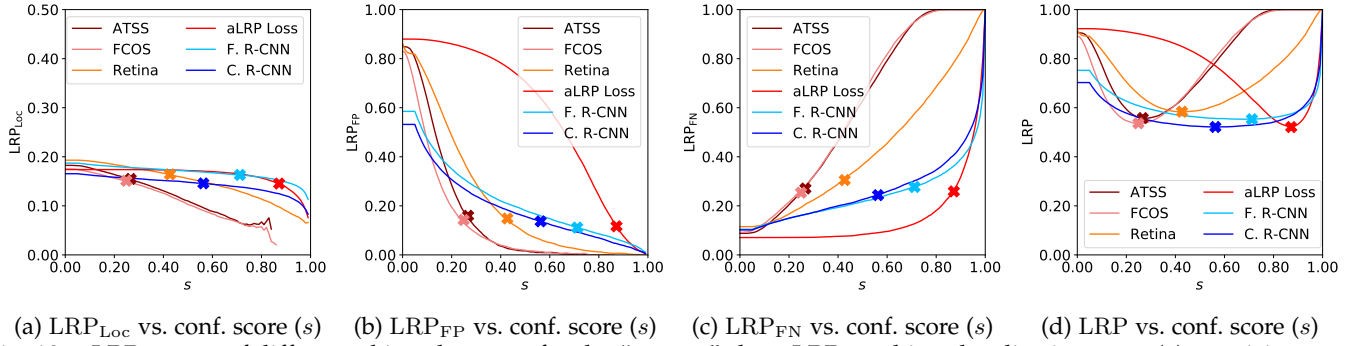
Firstly, to see why visual object detectors can be sensitive to thresholding, Figure 10 shows on the “person” class how performance (in terms of LRP and its components) evolves with different score thresholds (s) on different detectors. We observe in Figure 10(d) that the performances of some detectors (e.g. ATSS, FCOS, aLRP Loss) improve and degrade rapidly around s^* , a situation which implies the sensitivity of these detectors with respect to the threshold choice (i.e. model selection). For example, for ATSS, choosing a threshold larger than 0.50 has a significant impact on the performance, and even a threshold larger than 0.75 results in a detector with no TPs. Therefore, model selection is important for practical usage of object detectors.

Secondly, for a given detector, the variance of the LRP-Optimal thresholds over classes can be large (Figure 11- especially see RetinaNet in (b) and Cascade R-CNN in (d)). Thus, a general, fixed threshold for all classes can not provide optimal performance for all classes. Class-specific thresholding is required for optimal performance of visual object detectors.

Based on these observations, in Appendix H, we present a use-case of LRP-Optimal Thresholds on a video object detector which, first, collects thresholded detections from a conventional object detector, and then associates detection results between frames. On this use-case, we show that using class-specific LRP-Optimal thresholds significantly improves performance (up to around 9 points AP_{50} and 4 points oLRP) compared to using general, class-independent thresholding.

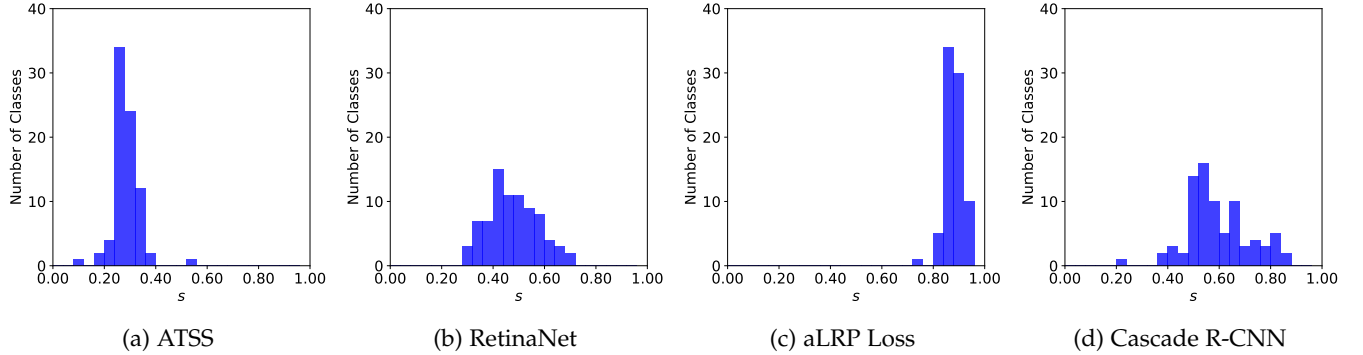
8 CONCLUSION

In this paper, we introduced a novel performance metric, LRP Error, to evaluate *all* visual detection tasks as an alternative to the widely-used measures AP and PQ. LRP Error has a number of advantages which we demonstrated in the paper: LRP Error (i) is “complete” in the sense that it precisely takes into account all important performance aspects (i.e. localization quality, recall, precision) of visual object detectors, (ii) is easily interpretable through its components, and (iii) does not suffer from the practical drawbacks of AP and PQ.



(a) LRP_{Loc} vs. conf. score (s) (b) LRP_{FP} vs. conf. score (s) (c) LRP_{FN} vs. conf. score (s) (d) LRP vs. conf. score (s)

Fig. 10: s -LRP curves of different object detectors for the “person” class. LRP combines localisation error (a), precision error (b) and recall error (c) over entire s domain in (d). The minimum-achievable LRP error in (d) is coined as oLRP (i.e. marked by “x”). Note that for some detectors (e.g. ATSS), the performance with respect to s changes abruptly in (d), hence, for some object detectors, the performance is very sensitive to thresholding. The lines with a different red tone represent a one-stage detector, while blue tones correspond to two-stage detector F. R-CNN: Faster R-CNN, C. R-CNN: Cascade R-CNN



(a) ATSS (b) RetinaNet (c) aLRP Loss (d) Cascade R-CNN

Fig. 11: The distributions of the class-specific LRP-Optimal Thresholds (s^*) for different methods. The variance of the LRP-Optimal thresholds can be large among classes. Thus, using a single general threshold for all classes will provide sub-optimal results.

Appendices: This paper is accompanied with appendices, containing the definitions of the frequently used terms and notation; proofs showing that PQ is not a metric but LRP is; a discussion on weighting LRP Error due to practical needs; why average LRP is not suitable as a performance metric; the derivation of the similarity of PQ and LRP; the repositories of the models; and more experiments on using LRP-Optimal thresholds in a use-case, analysing the latency of LRP computation and analysing the effect of the TP validation threshold on LRP.

ACKNOWLEDGMENTS

This work was supported by the Scientific and Technological Research Council of Turkey (TÜBİTAK) through project called “Object Detection in Videos with Deep Neural Networks” (project no 117E054). We also gratefully acknowledge (i) the support of NVIDIA Corporation with the donation of the Tesla K40 GPU and (ii) the computational resources kindly provided by Roketsan Missiles Inc. used for this research. Kemal Oksuz is supported by the TÜBİTAK 2211-A National Scholarship Programme for Ph.D. students.

REFERENCES

- [1] T.-Y. Lin, M. Maire, S. Belongie, J. Hays, P. Perona, D. Ramanan, P. Dollár, and C. L. Zitnick, “Microsoft COCO: Common Objects in Context,” in *The European Conference on Computer Vision (ECCV)*, 2014.
- [2] O. Russakovsky, J. Deng, H. Su, J. Krause, S. Satheesh, S. Ma, Z. Huang, A. Karpathy, A. Khosla, M. Bernstein, A. C. Berg, and L. Fei-Fei, “Imagenet large scale visual recognition challenge,” *International Journal of Computer Vision (IJCV)*, vol. 115, no. 3, pp. 211 – 252, 2015.
- [3] M. Everingham, L. Van Gool, C. K. I. Williams, J. Winn, and A. Zisserman, “The pascal visual object classes (voc) challenge,” *International Journal of Computer Vision (IJCV)*, vol. 88, no. 2, pp. 303–338, 2010.
- [4] S. Shao, Z. Li, T. Zhang, C. Peng, G. Yu, X. Zhang, J. Li, and J. Sun, “Objects365: A large-scale, high-quality dataset for object detection,” in *The IEEE International Conference on Computer Vision (ICCV)*, 2019.
- [5] M. Cordts, M. Omran, S. Ramos, T. Rehfeld, M. Enzweiler, R. Benenson, U. Franke, S. Roth, and B. Schiele, “The cityscapes dataset for semantic urban scene understanding,” in *IEEE Conference on Computer Vision and Pattern Recognition (CVPR)*, 2016.
- [6] A. Kuznetsova, H. Rom, N. Alldrin, J. R. R. Uijlings, I. Krasin, J. Pont-Tuset, S. Kamali, S. Popov, M. Mallocci, T. Duerig, and V. Ferrari, “The open images dataset V4: unified image classification, object detection, and visual relationship detection at scale,” arXiv e-prints:1811.00982, 2018.
- [7] A. Gupta, P. Dollar, and R. Girshick, “Lvis: A dataset for large vocabulary instance segmentation,” in *The IEEE Conference on Computer Vision and Pattern Recognition (CVPR)*, 2019.
- [8] K. Oksuz, B. C. Cam, E. Akbas, and S. Kalkan, “Localization recall precision (LRP): A new performance metric for object detection,” in *The European Conference on Computer Vision (ECCV)*, 2018.
- [9] A. Kirillov, K. He, R. Girshick, C. Rother, and P. Dollar, “Panoptic segmentation,” in *The IEEE Conference on Computer Vision and Pattern Recognition (CVPR)*, June 2019.
- [10] D. Hall, F. Dayoub, J. Skinner, H. Zhang, D. Miller, P. Corke, G. Carneiro, A. Angelova, and N. Suenderhauf, “Probabilistic object detection: Definition and evaluation,” in *Proceedings of the*

- IEEE/CVF Winter Conference on Applications of Computer Vision (WACV), 2020.
- [11] Y. Wu, A. Kirillov, F. Massa, W.-Y. Lo, and R. Girshick, "Detectron2," <https://github.com/facebookresearch/detectron2>, (Last accessed: 10 July 2020).
 - [12] F. Bourgeois and J.-C. Lassalle, "An extension of the munkres algorithm for the assignment problem to rectangular matrices," *Communications of ACM*, vol. 14, no. 12, pp. 802–804, 1971.
 - [13] D. Hoiem, Y. Chodpathumwan, and Q. Dai, "Diagnosing error in object detectors," in *The IEEE European Conference on Computer Vision (ECCV)*, 2012.
 - [14] D. Bolya, S. Foley, J. Hays, and J. Hoffman, "Tide: A general toolbox for identifying object detection errors," in *The IEEE European Conference on Computer Vision (ECCV)*, 2020.
 - [15] D. Schuhmacher, B. T. Vo, and B. N. Vo, "A consistent metric for performance evaluation of multi-object filters," *IEEE Transactions on Signal Processing*, vol. 56, no. 8, pp. 3447–3457, 2008.
 - [16] K. Oksuz and A. T. Cemgil, "Multitarget tracking performance metric: deficiency aware subpattern assignment," *IET Radar, Sonar Navigation*, vol. 12, no. 3, pp. 373–381, 2018.
 - [17] K. Chen, J. Wang, J. Pang, Y. Cao, Y. Xiong, X. Li, S. Sun, W. Feng, Z. Liu, J. Xu, Z. Zhang, D. Cheng, C. Zhu, T. Cheng, Q. Zhao, B. Li, X. Lu, R. Zhu, Y. Wu, J. Dai, J. Wang, J. Shi, W. Ouyang, C. Change Loy, and D. Lin, "MMDetection: Open MMLab Detection Toolbox and Benchmark," arXiv e-prints:1906.07155, 2019.
 - [18] Y. He, C. Zhu, J. Wang, M. Savvides, and X. Zhang, "Bounding box regression with uncertainty for accurate object detection," in *The IEEE Conference on Computer Vision and Pattern Recognition (CVPR)*, 2019.
 - [19] H. Qiu, H. Li, Q. Wu, and H. Shi, "Offset bin classification network for accurate object detection," in *IEEE/CVF Conference on Computer Vision and Pattern Recognition (CVPR)*, 2020.
 - [20] K. Oksuz, B. Can Cam, E. Akbas, and S. Kalkan, "A ranking-based, balanced loss function unifying classification and localisation in object detection," in *Advances in Neural Information Processing Systems (NeurIPS)*, 2020.
 - [21] Z. Cai and N. Vasconcelos, "Cascade R-CNN: Delving into high quality object detection," in *The IEEE Conference on Computer Vision and Pattern Recognition (CVPR)*, 2018.
 - [22] H. Rezatofighi, N. Tsoi, J. Gwak, A. Sadeghian, I. Reid, and S. Savarese, "Generalized intersection over union: A metric and a loss for bounding box regression," in *The IEEE Conference on Computer Vision and Pattern Recognition (CVPR)*, 2019.
 - [23] H. Zhang, H. Chang, B. Ma, N. Wang, and X. Chen, "Dynamic R-CNN: Towards high quality object detection via dynamic training," in *The European Conference on Computer Vision (ECCV)*, 2020.
 - [24] W. Liu, D. Anguelov, D. Erhan, C. Szegedy, S. E. Reed, C. Fu, and A. C. Berg, "SSD: single shot multibox detector," in *The European Conference on Computer Vision (ECCV)*, 2016.
 - [25] S. Ren, K. He, R. Girshick, and J. Sun, "Faster R-CNN: Towards real-time object detection with region proposal networks," *IEEE Transactions on Pattern Analysis and Machine Intelligence*, vol. 39, no. 6, pp. 1137–1149, 2017.
 - [26] J. Dai, Y. Li, K. He, and J. Sun, "R-FCN: Object detection via region-based fully convolutional networks," in *Advances in Neural Information Processing Systems (NeurIPS)*, 2016.
 - [27] C. Feichtenhofer, A. Pinz, and A. Zisserman, "Detect to track and track to detect," in *The IEEE International Conference on Computer Vision (ICCV)*, 2017.
 - [28] Y. Lu, C. Lu, and C. Tang, "Online video object detection using association lstm," in *IEEE International Conference on Computer Vision (ICCV)*, 2017.
 - [29] K. Chen, J. Li, W. Lin, J. See, J. Wang, L. Duan, Z. Chen, C. He, and J. Zou, "Towards accurate one-stage object detection with ap-loss," in *The IEEE Conference on Computer Vision and Pattern Recognition (CVPR)*, 2019.
 - [30] T. Lin, P. Goyal, R. B. Girshick, K. He, and P. Dollár, "Focal loss for dense object detection," in *The IEEE International Conference on Computer Vision (ICCV)*, 2017.
 - [31] Z. Tian, C. Shen, H. Chen, and T. He, "Fcos: Fully convolutional one-stage object detection," in *The IEEE International Conference on Computer Vision (ICCV)*, 2019.
 - [32] R. Girshick, I. Radosavovic, G. Gkioxari, P. Dollár, and K. He, "Detectron," <https://github.com/facebookresearch/detectron>, (Last accessed: 10 July 2020).
 - [33] H. Caesar, J. Uijlings, and V. Ferrari, "Coco-stuff: Thing and stuff classes in context," in *Proceedings of the IEEE Conference on Computer Vision and Pattern Recognition (CVPR)*, 2018.
 - [34] S. Zhang, C. Chi, Y. Yao, Z. Lei, and S. Z. Li, "Bridging the gap between anchor-based and anchor-free detection via adaptive training sample selection," in *IEEE/CVF Conference on Computer Vision and Pattern Recognition (CVPR)*, June 2020.
 - [35] G. Ghiasi, T. Lin, R. Pang, and Q. V. Le, "NAS-FPN: learning scalable feature pyramid architecture for object detection," in *The IEEE Conference on Computer Vision and Pattern Recognition (CVPR)*, 2019.
 - [36] B. Li, Y. Liu, and X. Wang, "Gradient harmonized single-stage detector," in *AAAI Conference on Artificial Intelligence*, 2019.
 - [37] X. Zhang, F. Wan, C. Liu, R. Ji, and Q. Ye, "Freeanchor: Learning to match anchors for visual object detection," in *Advances in Neural Information Processing Systems (NeurIPS)*, 2019.
 - [38] Z. Yang, S. Liu, H. Hu, L. Wang, and S. Lin, "Reppoints: Point set representation for object detection," in *The IEEE International Conference on Computer Vision (ICCV)*, 2019.
 - [39] J. Pang, K. Chen, J. Shi, H. Feng, W. Ouyang, and D. Lin, "Libra R-CNN: Towards balanced learning for object detection," in *The IEEE Conference on Computer Vision and Pattern Recognition (CVPR)*, 2019.
 - [40] X. Lu, B. Li, Y. Yue, Q. Li, and J. Yan, "Grid r-cnn," in *Proceedings of the IEEE Conference on Computer Vision and Pattern Recognition (CVPR)*, 2019.
 - [41] J. Wang, K. Chen, S. Yang, C. C. Loy, and D. Lin, "Region proposal by guided anchoring," in *The IEEE Conference on Computer Vision and Pattern Recognition (CVPR)*, 2019.
 - [42] K. He, G. Gkioxari, P. Dollár, and R. Girshick, "Mask R-CNN," in *The IEEE International Conference on Computer Vision (ICCV)*, 2017.
 - [43] Z. Huang, L. Huang, Y. Gong, C. Huang, and X. Wang, "Mask scoring r-cnn," in *IEEE Conference on Computer Vision and Pattern Recognition*, 2019.
 - [44] K. Chen, J. Pang, J. Wang, Y. Xiong, X. Li, S. Sun, W. Feng, Z. Liu, J. Shi, W. Ouyang, C. C. Loy, and D. Lin, "Hybrid task cascade for instance segmentation," in *IEEE/CVF Conference on Computer Vision and Pattern Recognition (CVPR)*, 2019.
 - [45] A. Kirillov, R. B. Girshick, K. He, and P. Dollár, "Panoptic feature pyramid networks," in *The IEEE Conference on Computer Vision and Pattern Recognition (CVPR)*, 2019.
 - [46] J. Deng, W. Dong, R. Socher, L.-J. Li, K. Li, and L. Fei-Fei, "ImageNet: A Large-Scale Hierarchical Image Database," in *The IEEE Conference on Computer Vision and Pattern Recognition (CVPR)*, 2009.
 - [47] K. Oksuz, B. C. Cam, E. Akbas, and S. Kalkan, "Ablation experiments repository of alrp loss," <https://github.com/kemaloksuz/aLRPLoss-AblationExperiments>, (Last accessed: 16 November 2020).
 - [48] Y. Wu and K. He, "Group normalization," in *The IEEE European Conference on Computer Vision (ECCV)*, 2018.
 - [49] K. J. Dembczynski, W. Waegeman, W. Cheng, and E. Hüllermeier, "An exact algorithm for f-measure maximization," in *Advances in Neural Information Processing Systems (NeurIPS)*, 2011.
 - [50] Z. C. Lipton, C. Elkan, and B. Naryanaswamy, "Optimal thresholding of classifiers to maximize f1 measure," in *Machine Learning and Knowledge Discovery in Databases*, 2014.
 - [51] S. Puthiya Parambath, N. Usunier, and Y. Grandvalet, "Optimizing f-measures by cost-sensitive classification," in *Advances in Neural Information Processing Systems (NeurIPS)*, 2014.
 - [52] E. Gundogdu and A. A. Alatan, "Good features to correlate for visual tracking," *IEEE Transactions on Image Processing*, vol. 27, no. 5, pp. 2526–2540, 2018.

APPENDICES

A FREQUENTLY USED TERMS AND NOTATION

Table A.6 presents the notation used throughout the paper, and below is a list of frequently used terms.

Hard Prediction: A type of visual object detector output which identifies each object with (i) a set of identifiers to locate an object (e.g. bounding box, mask, keypoints), and (ii) its class label.

Soft Prediction: A type of visual object detector output which identifies each object with (i) a set of identifiers to

TABLE A.6: Frequently used notations in the paper.

Symbol	Denotes
AP^C	COCO-Style AP
AP_τ	AP when the TPs are validated from the $lq(\cdot, \cdot)$ threshold of τ
d	A detection such that $d \in \mathcal{D}$
d_g	A TP detection that matches ground truth g and qualifies for performance evaluation
\mathcal{D}	A set of detections
FN	False Negative
FP	False Positive
g	A ground truth such that $g \in \mathcal{G}$
\mathcal{G}	A set of ground truths
$lq(\cdot, \cdot)$	A localisation quality function. (e.g. $IoU_B(\cdot, \cdot)$)
N_{FN}	Number of FNs
N_{FP}	Number of FPs
N_{TP}	Number of TPs
s^*	LRP-Optimal confidence score
TP	True Positive
τ	TP validation threshold in terms of localisation quality

locate an object (e.g. bounding box, mask, keypoints), (ii) its class label and (iii) the confidence score of the prediction.

Bounding Box: A rectangle on the image. Formally, a bounding box, denoted by B , is generally represented by $[x_1, y_1, x_2, y_2]$ with (x_1, y_1) denoting the top-left corner and (x_2, y_2) the bottom-right corner, with the constraints $x_2 > x_1$ and $y_2 > y_1$.

Keypoint Set: A set of coordinates to represent an object on the image such that each element is a two tuple (x_i, y_i) identifying a keypoint of an object.

Segmentation Mask: A set of pixels presenting which pixels belong to a particular object.

Intersection Over Union (IoU): For two polygons P_g and P_d , Intersection over Union (IoU) [3], [46], $IoU(P_g, P_d)$ is defined as :

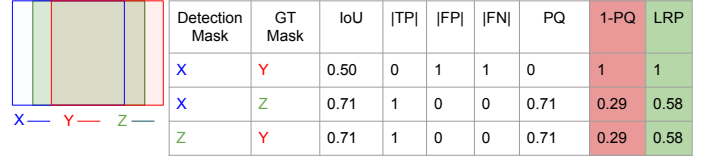
$$IoU(P_g, P_d) = \frac{A(P_g \cap P_d)}{A(P_g \cup P_d)}, \quad (A.10)$$

where $A(P)$ is the area of the polygon P (i.e. number of pixels delimited by P). These polygons are represented by bounding boxes for object detection, and by masks for segmentation tasks (e.g. instance segmentation, panoptic segmentation). $IoU \in [0, 1]$ and it is used to evaluate the localisation quality of a detection bounding box/mask with respect to its ground truth box/mask.

Object Keypoint Similarity (OKS): Given target and estimated keypoint sets, K_g and K_d respectively, with $k_g^i \in K_g$ and $k_d^i \in K_d$ being the i th keypoint of the object represented by a 2D coordinate on the image, Object Keypoint Similarity (OKS) [1] between k_g^i and k_d^i , denoted by $OKS(k_g^i, k_d^i)$, is

$$OKS(k_g^i, k_d^i) = \frac{\exp(-\|k_g^i - k_d^i\|^2)}{2(S\kappa^i)^2}, \quad (A.11)$$

where $\|\cdot\|$ is Euclidean distance, κ^i is the constant corresponding to i th keypoint to control falloff, and S is the object scale (e.g. the area of the ground truth bounding box divided by the total image area). Then, OKS between K_g and K_d , $OKS(K_g, K_d)$, is simply the average of $OKS(k_g^i, k_d^i)$ over



Detection Mask	GT Mask	IoU	TP	FP	FN	PQ	1-PQ	LRP
X	Y	0.50	0	1	1	0	1	1
X	Z	0.71	1	0	0	0.71	0.29	0.58
Z	Y	0.71	1	0	0	0.71	0.29	0.58

Fig. A.12: A counter-example which shows that PQ Error (i.e., 1-PQ) violates triangle inequality. Hence, PQ Error is not a metric. (a) Three different inputs (i.e. masks) X , Y and Z . (b) $1 - PQ$ does not satisfy the triangle inequality (i.e. $1 - PQ(X, Y) > 1 - PQ(X, Z) + 1 - PQ(Z, Y)$), while LRP does (i.e. $LRP(X, Y) \leq LRP(X, Z) + LRP(Z, Y)$). See Table A.6 for the notation.

single keypoints annotated in the dataset:

$$OKS(K_g, K_d) = \frac{1}{|K_g|} \sum_{i \in |K_g|} OKS(k_g^i, k_d^i). \quad (A.12)$$

Similar to $IoU(\cdot, \cdot)$; $OKS(\cdot, \cdot) \in [0, 1]$ and a larger $OKS(\cdot, \cdot)$ implies better localisation quality.

B PROOF THAT PQ ERROR IS NOT A METRIC

Here, we prove that PQ Error (i.e. (1-PQ)) is not a metric due to the fact that PQ Error violates triangle inequality⁵:

Theorem A.1. *PQ Error, defined by $1 - PQ(\mathcal{G}, \mathcal{D})$, violates triangle inequality, and hence it is not a metric.*

Proof. This is a proof by counter-example. If $1 - PQ(\mathcal{G}, \mathcal{D})$ satisfied triangle inequality, then we would expect $\forall \mathcal{A} \forall \mathcal{B} \forall \mathcal{C} \ 1 - PQ(\mathcal{A}, \mathcal{B}) \leq 1 - PQ(\mathcal{A}, \mathcal{C}) + 1 - PQ(\mathcal{C}, \mathcal{B})$. However, Figure A.12 presents a counterexample, therefore PQ Error ($1 - PQ(\mathcal{G}, \mathcal{D})$) violates triangle inequality and it is not a metric. \square

C PROOF THAT LRP IS A METRIC

In this section, we prove that, unlike PQ Error (Section B), LRP Error is a metric if the localisation error is a metric (i.e. $1 - lq(\cdot, \cdot)$). In our proof, we obtain LRP Error using a reduction from Deficiency Aware Subpattern Assignment (DASA) performance metric [16] from point multitarget tracking literature. Note that DASA is a proven metric.

Theorem A.2. *LRP is a metric.*

Proof. DASA metric is defined as:

$$\bar{e}_p^{(c)}(\mathcal{G}, \mathcal{D}) := \frac{l}{Z} \left(\frac{N_{TP}}{l} \left(\frac{1}{N_{TP}} \sum_{i=1}^{|\mathcal{G}|} \mathbb{I}[d(g_i, d_{g_i}) < c] d(g_i, d_{g_i})^p \right) + \left(\frac{c^p N_{FP}}{l} \right) + \left(\frac{c^p N_{FN}}{l} \right) \right)^{1/p}, \quad (A.13)$$

where $l = \max(\mathcal{G}, \mathcal{D})$, $Z = N_{TP} + N_{FP} + N_{FN}$, $\mathbb{I}[\cdot]$ is the indicator function, $d(g_i, d_{g_i})$ is an arbitrary metric, c is the cut-off length to validate TPs (i.e. TP assignment threshold)

⁵ PQ satisfies the other two metricity conditions, i.e. reflexivity and symmetry.

based on $d(g_i, d_{g_i})$, and finally p is the lp-norm parameter (see Table A.6 for the rest of the notation).

First, we set the lp-norm parameter, p , as 1 and simplify the definition:

$$\frac{1}{Z} \left(\left(\sum_{i=1}^{|G|} \mathbb{I}[d(g_i, d_{g_i}) < c] d(g_i, d_{g_i}) \right) + cN_{FP} + cN_{FN} \right). \quad (\text{A.14})$$

Second, we incorporate the TP validation criterion of visual object detectors in Equation A.14 as follows. A TP is identified if a ground truth, g_i , has a corresponding detection d_{g_i} such that $\text{lq}(g_i, d_{g_i}) > \tau$. Note that $\text{lq}(g_i, d_{g_i}) \in [0, 1]$. Then, to have a lower-better criterion which fits into Equation A.14, we can rewrite this TP validation criterion as $1 - \text{lq}(g_i, d_{g_i}) < 1 - \tau$. Having obtained the TP criterion, we set $d(g_i, d_{g_i}) = 1 - \text{lq}(g_i, d_{g_i})$ and $c = 1 - \tau$ in Equation A.14:

$$\frac{1}{Z} \left(\left(\sum_{i=1}^{|G|} \mathbb{I}[1 - \text{lq}(g_i, d_{g_i}) < 1 - \tau] (1 - \text{lq}(g_i, d_{g_i})) \right) + (1 - \tau)N_{FP} + (1 - \tau)N_{FN} \right), \quad (\text{A.15})$$

which can be rewritten by simplifying the predicate of $\mathbb{I}[\cdot]$ as follows:

$$\frac{1}{Z} \left(\left(\sum_{i=1}^{|G|} \mathbb{I}[\text{lq}(g_i, d_{g_i}) > \tau] (1 - \text{lq}(g_i, d_{g_i})) \right) + (1 - \tau)N_{FP} + (1 - \tau)N_{FN} \right). \quad (\text{A.16})$$

Next, we just simplify Equation A.16 in two steps: (i) We remove the Iverson Bracket by replacing $|G|$ by N_{TP} in the summation,

$$\frac{1}{Z} \left(\left(\sum_{i=1}^{N_{TP}} (1 - \text{lq}(g_i, d_{g_i})) \right) + (1 - \tau)N_{FP} + (1 - \tau)N_{FN} \right), \quad (\text{A.17})$$

and (ii) finally, noting that dividing by a constant does not violate metricity, in order to ensure the upper bound to be 1 and facilitate the interpretation of LRP, we divide Equation A.17 by $1 - \tau$:

$$\frac{1}{Z} \left(\sum_{i=1}^{N_{TP}} \frac{1 - \text{lq}(g_i, d_{g_i})}{1 - \tau} + N_{FP} + N_{FN} \right) = \text{LRP}(\mathcal{G}, \mathcal{D}). \quad (\text{A.18})$$

To conclude, LRP can be reduced from DASA, a proven metric, and therefore LRP is a metric. \square

D WEIGHTING THE COMPONENTS OF THE LRP ERROR FOR PRACTICAL NEEDS OF DIFFERENT APPLICATIONS

LRP Error does not give priority to any of the performance aspects (FP rate, FN rate and localisation error) and weights each performance aspect by considering their maximum possible contribution to the total matching error (Section 5.1 in the paper). On the other hand, depending on the requirements in a given application, one of the performance aspects can be given an emphasis. To illustrate a use-case, an online

video object detector may want to gather as much detections as it can after discarding the “noisy” examples of the still image detector. Note that removing the noisy examples still requires some thresholding, however, the conventional LRP-Optimal threshold, balancing the contribution of FPs and FNs, may not be the best solution to fulfill this requirement, and a lower threshold can be more suitable. In a different use-case, different weights for the components can also be beneficial for evaluation as well. For example, a ballistic missile detector may not tolerate FNs but can accept more FPs errors. To this end, Equation A.19 presents a weighted form of LRP Error:

$$\frac{1}{Z} \left(\sum_{i=1}^{N_{TP}} \alpha_{TP} \frac{1 - \text{lq}(g_i, d_{g_i})}{1 - \tau} + \alpha_{FP} N_{FP} + \alpha_{FN} N_{FN} \right), \quad (\text{A.19})$$

where $Z = \alpha_{TP} N_{TP} + \alpha_{FP} N_{FP} + \alpha_{FN} N_{FN}$, and α_{TP} , α_{FP} and α_{FN} correspond to the “importance weights” of each performance aspect. Following the interpretation of LRP (see Section 5), the importance weights imply duplicating each error by the value of this weight. Accordingly, they are included both in the “total matching error” (i.e. nominator) and the “maximum possible value of the total matching error” (i.e. normalisation constant). In order to increase the contribution of a component, the importance weight of the desired component is to be set larger than 1 (e.g. to double the contribution of false negatives, then $\alpha_{FN} = 2$ and $\alpha_{TP} = \alpha_{FP} = 1$). Note that when $\alpha_{TP} = \alpha_{FP} = \alpha_{FN} = 1$, Equation A.19 reduces to the conventional definition of LRP (Equation 2 in the paper). Finally, we note that this modification naturally violates the symmetry of the metric properties when $\alpha_{FP} \neq \alpha_{FN}$.

E WHY AVERAGE LRP (aLRP) IS NOT AN IDEAL PERFORMANCE MEASURE?

This section discusses why the recently proposed loss function aLRP Loss [20] is not an ideal performance measure.

Having a similar intuition to oLRP, we define aLRP Error by averaging the LRP Errors over the confidence scores (see Table A.6 for the notation):

$$\text{aLRP} := \frac{1}{|S|} \sum_{s \in S} \text{LRP}(\mathcal{G}, \mathcal{D}_s). \quad (\text{A.20})$$

where \mathcal{D}_s is the set of detections thresholded at confidence score s (i.e. those detections with larger confidence scores than s are kept, and others are discarded). However, without any improvement in the detection performance, aLRP Error can be reduced to oLRP Error with the following two steps:

- 1) Delete all the detections with $s < s^*$ from the detection output,
- 2) Set the confidence score of the remaining detections to 1.00.

This two-step simple algorithm will make the s-LRP curve to be a line determined by $s = s^*$ (see Figure 4(c) in the paper), and averaging over the confidence scores will yield oLRP. As a result, considering the fact that the performance with respect to aLRP is affected without any improvement in the detection performance, we do not prefer aLRP Error as a performance measure.

F THE SIMILARITY BETWEEN PQ AND LRP ERRORS

In this section, we derive Equation 8 in the original paper:

$$1 - \text{PQ} = \frac{1}{\hat{Z}} \left(\sum_{i=1}^{N_{\text{TP}}} \frac{1 - \text{lq}(g_i, d_{g_i})}{1 - 0.50} + N_{\text{FP}} + N_{\text{FN}} \right), \quad (\text{A.21})$$

where $\hat{Z} = 2N_{\text{TP}} + N_{\text{FP}} + N_{\text{FN}}$. LRP and PQ Errors are very similar: Removing 2 (in red) from \hat{Z} yields $1 - \text{PQ} = \text{LRP}$.

Recall from Equation 1 in the paper that PQ is defined as (see Table A.6 for the notation):

$$\text{PQ}(\mathcal{G}, \mathcal{D}) = \frac{1}{N_{\text{TP}} + \frac{1}{2}N_{\text{FP}} + \frac{1}{2}N_{\text{FN}}} \left(\sum_{i=1}^{N_{\text{TP}}} \text{IoU}(g_i, d_{g_i}) \right). \quad (\text{A.22})$$

First, we replace $\text{IoU}(\cdot, \cdot)$ in Equation A.22 by $\text{lq}(\cdot, \cdot)$ to align the definitions of LRP and PQ:

$$\text{PQ}(\mathcal{G}, \mathcal{D}) = \frac{1}{N_{\text{TP}} + \frac{1}{2}N_{\text{FP}} + \frac{1}{2}N_{\text{FN}}} \left(\sum_{i=1}^{N_{\text{TP}}} \text{lq}(g_i, d_{g_i}) \right). \quad (\text{A.23})$$

Then, just by simple algebraic operations, we manipulate Equation A.23:

$$\text{PQ} = 1 - 1 + \frac{\sum_{i=1}^{N_{\text{TP}}} \text{lq}(g_i, d_{g_i})}{N_{\text{TP}} + \frac{1}{2}N_{\text{FP}} + \frac{1}{2}N_{\text{FN}}} \quad (\text{A.24})$$

$$= 1 - \left(1 - \frac{\sum_{i=1}^{N_{\text{TP}}} \text{lq}(g_i, d_{g_i})}{N_{\text{TP}} + \frac{1}{2}N_{\text{FP}} + \frac{1}{2}N_{\text{FN}}} \right) \quad (\text{A.25})$$

$$= 1 - \frac{N_{\text{TP}} + \frac{1}{2}N_{\text{FP}} + \frac{1}{2}N_{\text{FN}} - \sum_{i=1}^{N_{\text{TP}}} \text{lq}(g_i, d_{g_i})}{N_{\text{TP}} + \frac{1}{2}N_{\text{FP}} + \frac{1}{2}N_{\text{FN}}} \quad (\text{A.26})$$

$$= 1 - \frac{N_{\text{TP}} - \sum_{i=1}^{N_{\text{TP}}} \text{lq}(g_i, d_{g_i}) + \frac{1}{2}N_{\text{FP}} + \frac{1}{2}N_{\text{FN}}}{N_{\text{TP}} + \frac{1}{2}N_{\text{FP}} + \frac{1}{2}N_{\text{FN}}} \quad (\text{A.27})$$

$$= 1 - \frac{\sum_{i=1}^{N_{\text{TP}}} 1 - \sum_{i=1}^{N_{\text{TP}}} \text{lq}(g_i, d_{g_i}) + \frac{1}{2}N_{\text{FP}} + \frac{1}{2}N_{\text{FN}}}{N_{\text{TP}} + \frac{1}{2}N_{\text{FP}} + \frac{1}{2}N_{\text{FN}}} \quad (\text{A.28})$$

$$= 1 - \frac{\sum_{i=1}^{N_{\text{TP}}} (1 - \text{lq}(g_i, d_{g_i})) + \frac{1}{2}N_{\text{FP}} + \frac{1}{2}N_{\text{FN}}}{N_{\text{TP}} + \frac{1}{2}N_{\text{FP}} + \frac{1}{2}N_{\text{FN}}} \quad (\text{A.29})$$

$$= 1 - \frac{1}{\hat{Z}} \left(\sum_{i=1}^{N_{\text{TP}}} \frac{1 - \text{lq}(g_i, d_{g_i})}{1 - 0.50} + N_{\text{FP}} + N_{\text{FN}} \right), \quad (\text{A.30})$$

where $\hat{Z} = 2N_{\text{TP}} + N_{\text{FP}} + N_{\text{FN}}$. As a result, we can rewrite Equation A.30 to express the PQ Error (i.e. $1 - \text{PQ}$) as follows:

$$1 - \text{PQ} = \frac{1}{\hat{Z}} \left(\sum_{i=1}^{N_{\text{TP}}} \frac{1 - \text{lq}(g_i, d_{g_i})}{1 - 0.50} + N_{\text{FP}} + N_{\text{FN}} \right) \quad (\text{A.31})$$

TABLE A.7: The repositories of models that we downloaded, evaluated and utilized for comparison in Section 7 in the paper. The only exception is aLRP Loss [20], for which we used our own implementation [47]. The models are listed in alphabetical order.

Repository	Method
mmdetection [17]	ATSS [34]
	Cascade Mask R-CNN [21]
	Cascade R-CNN [21]
	FCOS [31]
	FreeAnchor [37]
	GHM [36]
	Grid R-CNN [40]
	Guided Anchoring [41]
	Hybrid Task Cascade [44]
	Libra R-CNN [39]
	Mask R-CNN [42]
	Mask Scoring R-CNN [43]
	NAS-FPN [35]
detectron [32]	RPDet [38]
	SSD [24]
detectron2 [11]	Faster R-CNN [25]
	RetinaNet [30]
detectron2 [11]	Keypoint R-CNN
	Panoptic FPN [45]

G THE REPOSITORIES AND CONFIGURATIONS OF THE USED MODELS IN THE EXPERIMENTS

In order to ensure reproducibility and facilitate direct usage of our results, Table A.7 associates the models with the three commonly-used repositories (i.e. detectron [32], detectron [11] and mmdetection [17]) from which we downloaded the trained models. The only exception is aLRP Loss [20], for which we used our own implementation [47]. For rare cases, there may be multiple alternatives for the same backbone and number of trained epochs owing to different design choices (e.g. using a different layer normalisation such as group normalisation [48]). In such cases, one can infer the corresponding model by comparing COCO-style AP values in the corresponding repository and Section 7 of the paper.

H MORE EXPERIMENTS

In addition to the experiments in our paper, here we demonstrate a use-case of LRP-Optimal Thresholds, and analyse the latency of LRP computation and the effect of TP validation threshold, τ , on LRP.

H.1 A Use-Case of LRP-Optimal Thresholds in Video Object Detection

Related Work on Setting the thresholds of the classifiers. Employing visual detectors for a practical application requires a confidence threshold that balances precision, recall and localisation performance since, otherwise, the resulting output would be dominated by several false positives with low confidence scores. However, this topic has not received

much attention from the research community and is usually handled by practitioners in a problem or deployment-specific manner. Conventionally, the thresholds of classifiers are set by finding the optimal F-measure on the PR curve or G-mean on the receiver operating characteristics curve, which do not consider localisation quality. Prior work on setting the classifier thresholds focused on the probabilistic models [49], [50]. Parambath et al. [51] present a theoretical analysis of the F-measure, and propose a practical algorithm discretizing the confidence scores in order to search for the optimal F-measure. Currently, for object detection, a general single threshold is used for all classes instead of class-specific thresholds [28].

The Experimental Setup. Here, we demonstrate a use-case where oLRP helps us to set class-specific optimal thresholds as an alternative to the naive approach of using a general, class-independent threshold. To this end, we develop a simple, online video object detection framework where we use an off-the-shelf still-image object detector (RetinaNet-50 [30] trained on COCO [1]) and built three different versions of the video object detector. The first version, denoted with B , uses the still-image object detector to process each frame of the video independently. The second and third versions, denoted with G and S , respectively, again use the still-image object detector to process each frame and in addition, they link bounding boxes across subsequent frames using the Hungarian matching algorithm [12] and update the scores of these linked boxes using a simple Bayesian rule (details of this simple online video object detector is given below). The only difference between G and S is that while G uses a validated threshold of 0.50 (see Figure 11(b) in the paper to notice that the LRP-Optimal Threshold distribution of RetinaNet has a mean around 0.50) as the confidence score threshold for all classes, S uses LRP-Optimal Threshold per class. We test these three detectors on 346 videos of ImageNet VID validation set [2] for 15 object classes which also happen to be included in COCO.

Details of the Online Video Object Detectors. There are two online video object detectors: G and S which respectively use the general, class-independent thresholding approach with 0.50 as threshold and the class-specific thresholds. For each of the online detectors, at each time interval, the detections from the previous and current frames are associated using the Hungarian algorithm [12] considering a box linking function and the confidence scores of associated BBs of the current frame are updated using the score distributions from both frames. Since an online tracker, specifically [52], is also used in our method, we use the L1 norm of the difference of confidence score distributions of neighbouring frames and the IoU overlap of the tracker prediction and the detection at current frame. While choosing this box linking function, we inspired from the tube linking score of [27]. The updated score is estimated using the Bayes Theorem such that the prior is the updated tubelet score in the previous frame and likelihood is the currently associated high confidence detection with that tubelet. In such an update method, even though the updated scores converge to 1 quickly, which is harmful for lower recall, precision improves in larger recall portions. Also, we call a BB as “dominant object” if its updated score increases by

0.20. In order to increase the recall, the disappearance of a “dominant object” is closely inspected by using the tracker again to predict the possible location, then the cropped region is classified by class-wise binary classifiers (object vs. background).

AP vs. oLRP for Video Object Detection: We compare G with B in order to represent the evaluation perspectives of AP and oLRP – see Figure A.13 and Table A.8. Since B is a conventional object detector, with conventional PR curves as illustrated in Figure A.13. On the other hand, in order to be faster, G ignores some of the detections causing its maximum recall to be less than that of B . Thus, these shorter ranges in the recall set a big problem in the evaluation with respect to AP. Quantitatively, B surpasses G by 7.5% AP. On the other hand, despite limited recall coverage, G obtains higher precision than B especially through the end of its PR curve. To illustrate, for the “boat” class in Figure A.13, G has significantly better precision after approximately between 0.5 and 0.9 recall even though its AP is lower by 6%. Since oLRP compares methods concerning their best configurations, this difference is clearly addressed comparing their oLRP error in which G surpasses S by 4.1%. Furthermore, the superiority of G is shown to be its higher precision since FN components of G and S are very close while FP component of G is 8.6% better, which is also the exact difference of precisions in their peaks of PR curves.

Therefore, while G seems to have very low performance in terms of AP, for 12 classes G reaches better peaks than B as illustrated by the oLRP values in Table A.8. This suggests that oLRP is better than AP in capturing the performance details of this kind methods that uses thresholding.

Effect of the Class-specific LRP-Optimal Thresholds: Compared to G , owing to the class-specific thresholds, S has 1.7% better AP and 0.5% better oLRP as shown in Table A.8. However, since the mean is dominated by s^* around 0.50, it is better to focus on classes with low or high s^* values in order to grasp the effect of the approach. The “bus” class has the lowest s^* with 27%. For this class, S surpasses G by 8.7% in AP and 3.9% in oLRP. This performance increase is also observed for other classes with very low thresholds, such as “airplane”, “bicycle” and “zebra”. For these classes with lower thresholds, the effect of LRP-Optimal threshold on the PR curve is to stretch the curve in the recall domain (maybe by accepting some loss in precision) as shown in the “bus” example in Figure A.13. Not surprisingly, “cow” is one of the two classes for which AP of S is lower since its threshold is the highest and thereby causing recall to be more limited. On the other hand, regarding oLRP, the result is not worse since this time the PR curve is stretched through the positive precision, as shown in Figure A.13, allowing better FP errors. Thus, in any case, lower or higher, the LRP-Optimal Threshold aims to discover the best PR curve. There are four classes in total for which G is better than S in terms of oLRP. However, note that the maximum difference is 0.2% in oLRP and these are the classes with thresholds around 0.5. These suggest that choosing class-specific thresholds rather than the general, class-independent thresholding approach increases the performance of the detector especially for classes with low or high class-specific thresholds.

TABLE A.8: Comparison among B , G , S with respect to AP & oLRP and their best class-specific configurations. The mean of class thresholds are assigned as N/A since the thresholds are set class-specific and the mean is not used. s^* denotes the LRP-Optimal Thresholds. Note that unlike AP, lower scores are better for LRP.

	Method	airplane	bicycle	bird	bus	car	cow	dog	cat	elephant	horse	motorcycle	sheep	train	boat	zebra	mean
AP ₅₀	B	68.1	63.0	54.7	56.5	55.5	58.7	46.3	60.1	66.1	47.3	60.2	56.1	71.3	82.9	81.6	61.9
	G	62.1	44.5	49.2	39.8	41.7	51.0	41.6	56.8	58.8	44.1	57.1	54.7	60.0	76.9	76.5	54.4
	S	64.5	53.5	50.0	48.5	41.9	49.2	43.4	56.9	58.9	44.4	57.3	54.5	60.9	79.2	78.2	56.1
oLRP	B	62.7	77.6	71.8	70.2	75.9	69.2	72.8	70.0	62.5	72.3	69.2	67.7	58.3	59.4	43.6	66.9
	G	60.6	78.3	69.1	72.7	75.8	67.9	71.4	69.7	61.4	69.9	65.4	64.8	58.6	55.3	43.2	65.6
	S	60.3	76.2	68.7	68.8	75.9	67.8	71.2	69.7	61.3	70.1	65.5	64.9	58.3	55.1	42.5	65.1
oLRP _{Loc}	B	18.2	27.1	16.9	17.7	20.7	14.5	16.6	20.3	17.0	15.5	19.2	15.4	15.9	19.9	12.8	17.9
	G	18.1	25.8	17.0	16.0	20.7	15.1	16.5	20.0	17.0	16.0	19.5	15.5	15.6	19.5	12.8	17.7
	S	18.6	27.0	17.0	17.3	20.7	14.8	17.0	20.0	17.0	16.0	19.4	15.5	15.9	19.7	13.1	17.9
oLRP _{FP}	B	8.0	22.8	30.0	20.3	30.3	22.4	24.2	24.8	9.5	24.6	15.8	14.1	9.9	16.3	3.4	18.4
	G	8.6	11.6	17.4	13.7	31.1	21.8	22.9	27.9	7.1	22.1	4.9	7.8	9.1	7.7	1.6	14.2
	S	8.7	22.6	18.4	19.3	32.0	18.2	26.9	28.3	7.5	23.1	8.4	7.8	11.0	8.9	3.0	16.3
oLRP _{FN}	B	38.3	42.7	47.8	47.7	49.9	50.4	53.3	39.4	39.5	54.0	44.8	49.4	34.4	22.4	22.0	42.4
	G	35.9	52.3	48.0	57.1	49.3	47.3	51.2	37.2	38.8	49.4	41.5	46.7	36.0	22.1	22.7	42.4
	S	32.6	38.9	48.9	46.1	48.8	49.0	48.0	36.9	38.5	49.3	40.6	46.8	33.9	20.3	20.2	39.8
s^*	B	0.38	0.31	0.44	0.27	0.49	0.61	0.42	0.49	0.49	0.52	0.45	0.51	0.41	0.45	0.31	N/A
	G	0.00	0.69	0.97	0.68	0.00	0.96	0.48	0.70	0.33	0.64	0.60	0.84	0.59	0.90	0.00	N/A
	S	0.00	0.54	0.98	0.45	0.00	0.91	0.49	0.64	0.39	0.58	0.63	0.85	0.55	0.89	0.54	N/A

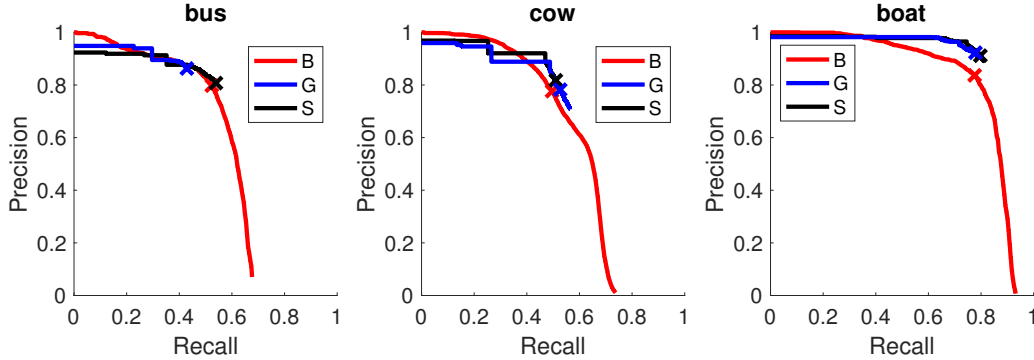


Fig. A.13: Example PR curves of the methods on three example classes. Optimal PR pairs are marked with crosses. Using a LRP-Optimal Threshold balances FP and FN errors resulting in a stretched PR curve either in recall (e.g.(a)) or precision (e.g.(b)) axis depending on the chosen general threshold. Furthermore, using AP for these pruned PR curves does not provide consistent performance evaluation.

H.2 Analysing Latency of LRP Computation

To evaluate soft predictions and hard predictions using LRP, we incorporated the corresponding LRP variant into the official COCO evaluation [1] and panoptic segmentation repositories [9] respectively. Since the PQ and LRP are very similar in formulation (Section 6 in the paper), it is obvious that they require very similar time to compute. Hence, in this section we focus on how much time computing LRP adds to the AP computation.

During the computation of AP, COCO evaluation follows a five-step algorithm: (i) loading annotations into memory, (ii) loading and preparing results, (iii) per image evaluation, (iv) accumulating evaluation results, and (v) summarizing (i.e. printing) the results. Since step (i) and (ii) are independent of the performance measure, and (v) is a simple printing operation (i.e. it takes less than 3 seconds compute (i), (ii) and (v) in total) and we do not change (iii) per image

evaluation except returning the computed IoUs of TPs, we analysed the additional latency of computing oLRP for step (iv) accumulation, in which the per-image evaluation results are combined into performance values. In order to do that using a standard CPU, we computed and averaged the runtime of this step using all 32 SOTA models in Table 3 in the paper on COCO *minival* with 5000 images. We observed that LRP computation (including LRP, oLRP, their components, class-specific LRP-Optimal Thresholds for different “size” and “maximum detection number” criteria as done by COCO toolkit - see [1] for details) introduces a negligible overhead with around one second both for (iv) accumulate step (from 5.8 seconds to 6.6 seconds) and for entire computation (from 38.7 to 39.6 seconds).

H.3 Analyzing the Effect of TP Validation Threshold

Finally, we analyse how LRP is affected from the TP validation threshold parameter, τ . We use Faster R-CNN (X101-12)

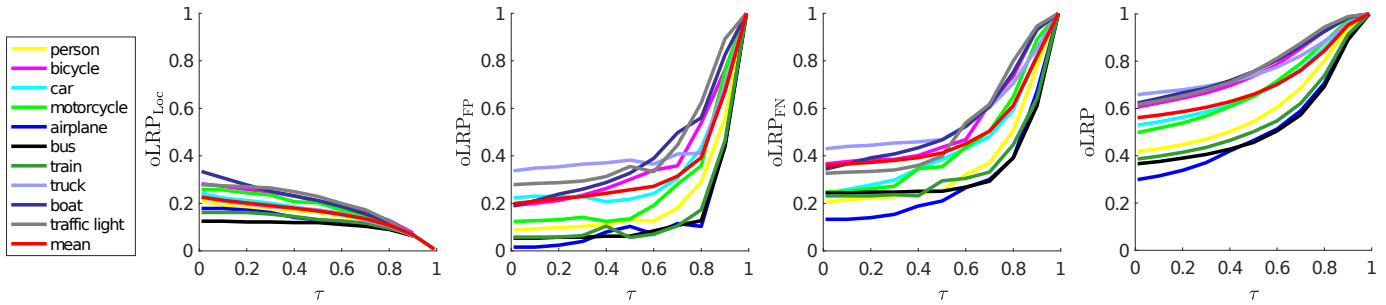


Fig. A.14: For each class, oLRP and its components for Faster R-CNN (X101-12) are plotted against τ . The mean represents the mean of 80 classes.

(Table 3 in the paper) results of the first 10 classes and mean-error for clarity, the effect of the τ parameter is analysed in Figure A.14 on oLRP. As expected, larger τ values imply lower localisation error (oLRP_{Loc}). On the other hand, a larger τ causes FP and FN components to increase rapidly, leading to higher total error (oLRP). This is intuitive since at the extreme case, i.e., when $\tau = 1$, there are hardly any TP (i.e. all the detections are FPs), which makes oLRP to be 1. Therefore, LRP allows measuring the performance of a detector designed for an application that requires a different τ by also providing additional information. In addition, investigating oLRP for different τ values represents a good extension for ablation studies.



Emre Akbas is an assistant professor at the Department of Computer Engineering, Middle East Technical University (METU), Ankara, Turkey. He received his Ph.D. degree from the Department of Electrical and Computer Engineering, University of Illinois at Urbana-Champaign in 2011. His M.Sc. and B.Sc. degrees in computer science are both from METU. Prior to joining METU, he was a postdoctoral research associate at the Department of Psychological and Brain Sciences, University of California Santa Barbara. His research interests are in computer vision and deep learning with a focus on object detection and human pose estimation.

search interests are in computer vision and deep learning with a focus on object detection and human pose estimation.



Kemal Oksuz received B.Sc. in System Engineering from Land Forces Academy of Turkey in 2008 and his M.Sc. in Computer Engineering in 2016 from Bogazici University with high honor degree. He is currently pursuing his Ph.D. in Middle East Technical University, Ankara, Turkey. His research interests include computer vision with a focus on object detection.



Baris Can Cam received his B.Sc. degree in Electrical and Electronics Engineering from Eskişehir Osmangazi University, Turkey in 2016. He is currently pursuing his M.Sc. in Middle East Technical University, Ankara, Turkey. His research interests include computer vision with a focus on object detection.



Sinan Kalkan received his M.Sc. degree in Computer Engineering from Middle East Technical University (METU), Turkey in 2003, and his Ph.D. degree in Informatics from the University of Göttingen, Germany in 2008. After working as a postdoctoral researcher at the University of Göttingen and at METU, he became an assistant professor at METU in 2010. Since 2016, he has been working as an associate professor on problems within Computer Vision, and Developmental Robotics.